FIGURE S1, related to Figure 1

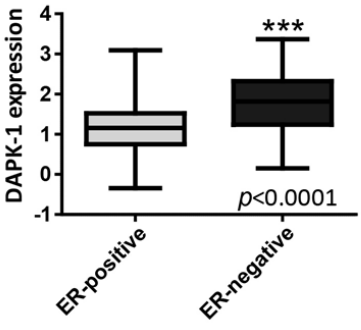

Desmedt dataset:
Publish: Clin Cancer Res 2007
Sample: 198 samples (64 ER-neg, 134 ER-pos

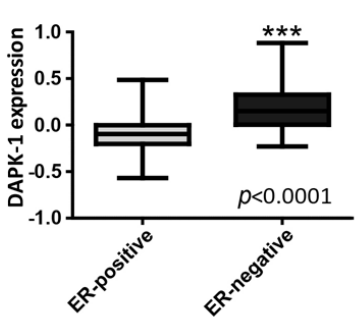

van de Vijver dataset:
Publish: N Engl J Med 2002
Sample: 295 samples (69-ER neg, 226-ER posi)

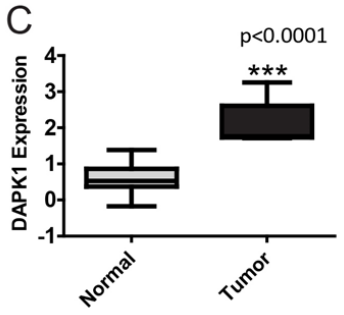

Karnoub Dataset
Publish: Nature 2007
Sample: 22 (15 Normal, 7 tumor)

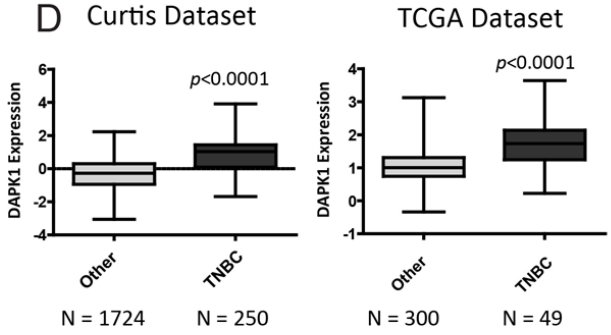

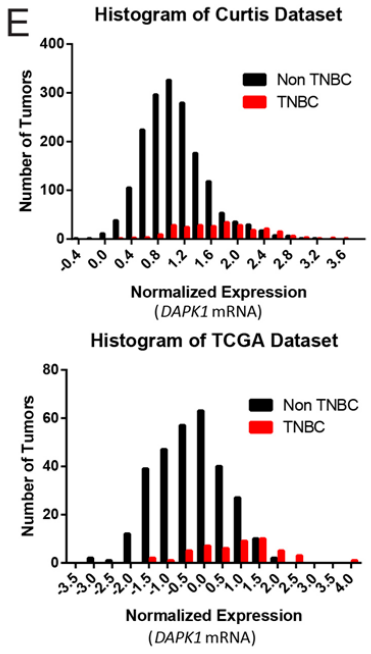

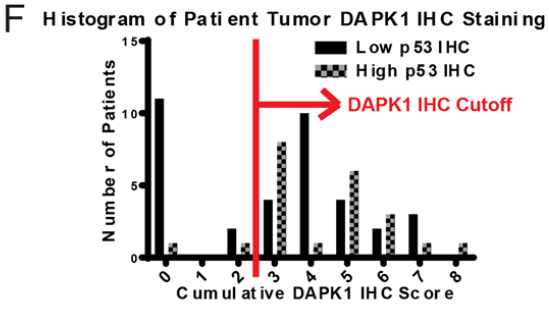

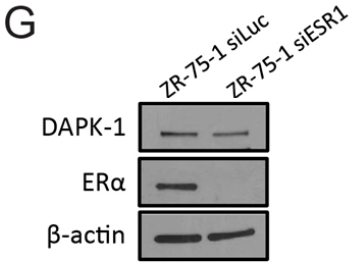

SF1: mRNA expression of DAPK1 in normal tissue vs. tumor and ER-positive vs. ER-negative breast tumor in public tumor datasets. **A)** mRNA expression of DAPK1 in ER-positive and ER-negative subtypes in Desmedt dataset (n=198) (1). **B)** mRNA expression of DAPK1 in ER-positive and ER-negative subtypes in van de Vijver Dataset (n=295) (2). **C)** mRNA expression of DAPK1 in normal and tumor samples in Karnoub Dataset (n=22) (3). Statistics analysis was performed using paired two-tailed *t-test*. **D)** mRNA expression for breast tumors in the Curtis (n=1699) and TCGA (n=390) (4-6) datasets stratified by TNBC status. **E)** DAPK1 expression histograms for the TNBC and non-TNBC populations overlayed for each of the Curtis et al and TCGA datasets demonstrating distinct population means. **F)** Breast cancer tissue microarray combined DAPK1 IHC histogramwith notation indicating the preselected threshold for positivity. **G)** Immunoblot analysis for estrogen receptor and DAPK1 in the ER(+), wt-p53 ZR 75-1 cell line. Cells were transfected with control siRNAs, siESR1 as indicated. *** indicates $p<0.0001$.

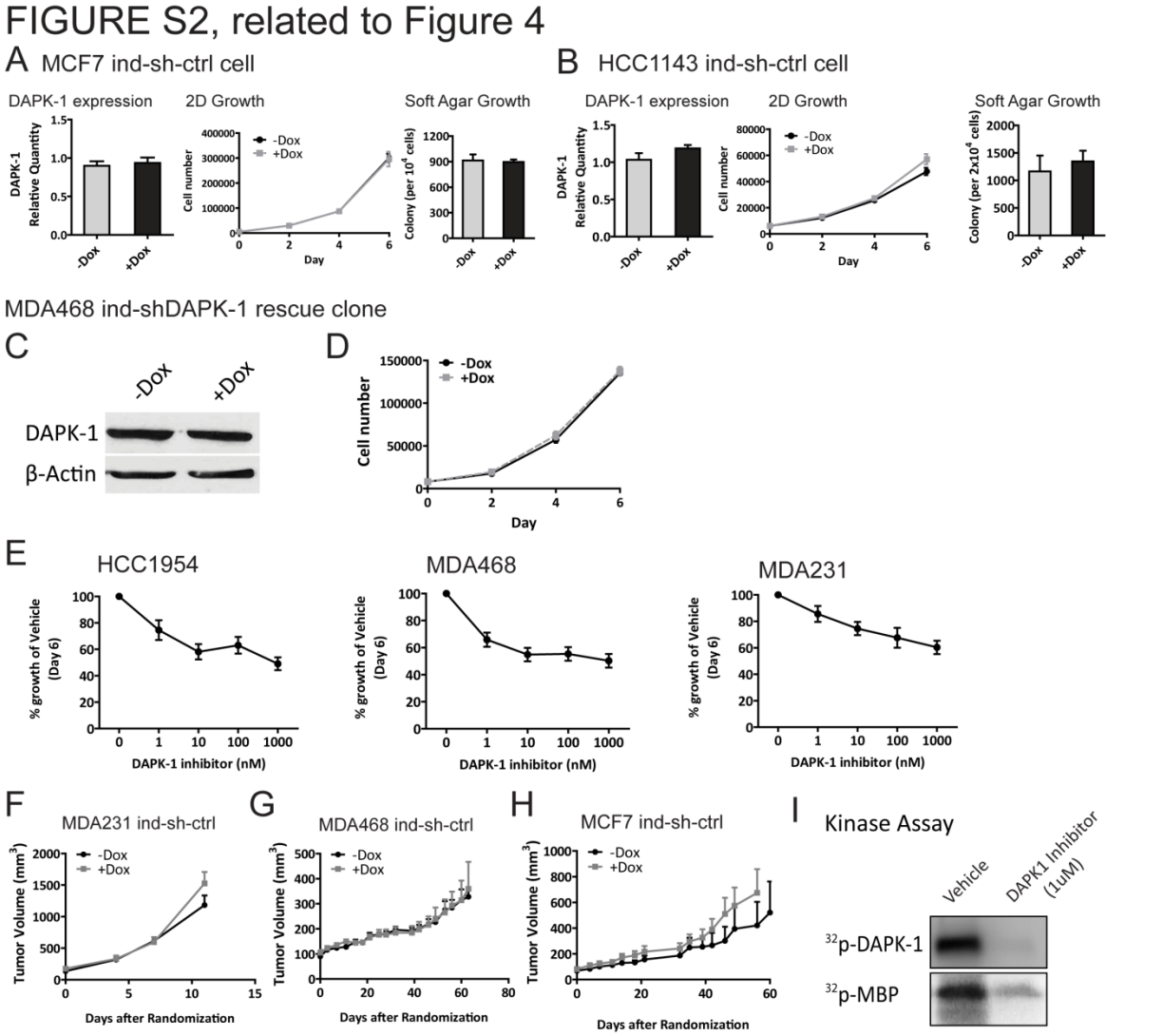

SF2: DAPK1 expression, 2D growth, anchorage-independent growth are not affected upon doxycycline addition in MCF7 and HCC1143 vector control cell lines. A) DAPK1 expression (Left), 2D growth (Middle) and anchorage-independent growth (Right) in MCF7 vector control cells before and after doxycycline addition. **B)** DAPK1 expression (Left), 2D growth (Middle) and anchorage-independent growth (Right) in HCC1143 vector control cells before and after doxycycline addition. Rescue of DAPK1 expression in MDA468 ind-shDAPK1 cells can restore the growth suppressive phenotype of DAPK1 depletion. **C)** DAPK1 expression in MDA468 ind-shDAPK1 with overexpressed DAPK1 before and after doxycycline addition. **D)** Growth curve of MDA468 ind-shDAPK1 with overexpressed DAPK1 before and after doxycycline addition. DAPK1 inhibitor suppresses the growth of ER-negative HCC1954, MDA468 and MDA231 in a gradient-dependent way. **E)** Response curve of HCC1954, MDA468 and MDA231 to DAPK1 inhibitor from 1nM to 1μM at day 6. Xenografts of vector control MDA231, MDA468 and MCF7 cells are not affected upon the addition of doxycycline. **F)** Xenograft growth of MDA231 ind-shctrl with and without doxycycline. **G)** Xenograft growth of MDA468 ind-shctrl with and without doxycycline. **H)** Xenograft growth of MCF7 ind-shctrl with and without doxycycline. **I)** In vitro kinase assay using purified DAPK1 protein and Myelin Basic Protein (MBP) as phosphorylation donors for DAPK1. Autoradiographs show the phosphorylated species at the expected molecular weights. DAPK1 knockdown and cell growth experiments were performed in triplicate, with results reported as average ± SEM. *indicates $p<0.01$ and **indicates $p<0.001$ by 2-tailed Student's *t* test.

FIGURE S3

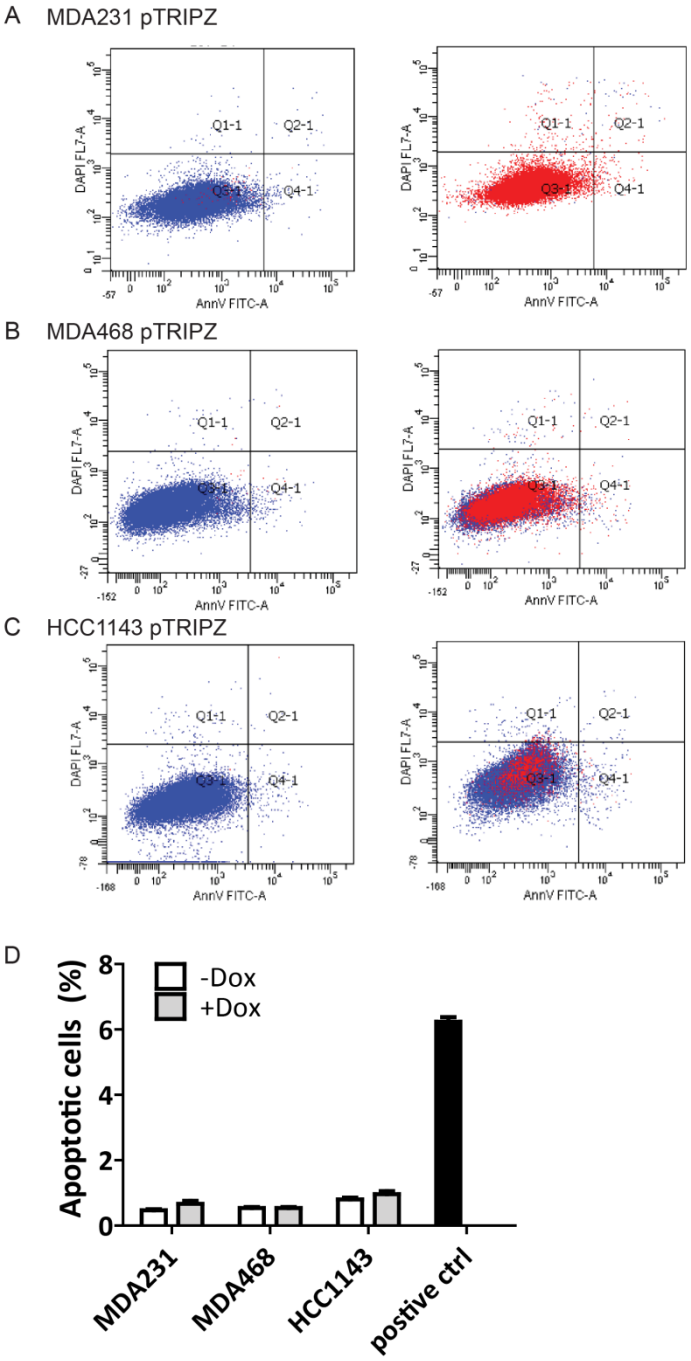

SF3: DAPK1 suppression does not induce apoptosis according to Annexin V-DAPI assay. MDA231 ind-shDAPK1, MDA468 ind-shDAPK1 and HCC1143 ind-shDAPK1 with and without doxycycline addition were submitted for FACS analysis with DAPI and Annexin-V staining. Annexin V+/DAPI- population represents early apoptotic cells while Annexin V+/DAPI+ population represents late apoptotic cells. **A)** Annexin V/DAPI staining of MDA231 ind-shDAPK1 cells without (**Left**) and with (**Right**) doxycycline addition. **B)** Annexin V/DAPI staining of MDA468 ind-shDAPK1 cells without (**Left**) and with (**Right**) doxycycline addition. **C)** Annexin V/DAPI staining of HCC1143 ind-shDAPK1 cells without (**Left**) and with (**Right**) doxycycline addition. **D)** Quantification of apoptotic rates in different cell lines. MDA231 cells treated with 12μM Camptothecin for 24h are served as positive control. Each data was performed in triplicate, with results reported as average ± SEM.

FIGURE S4, related to Figure 6

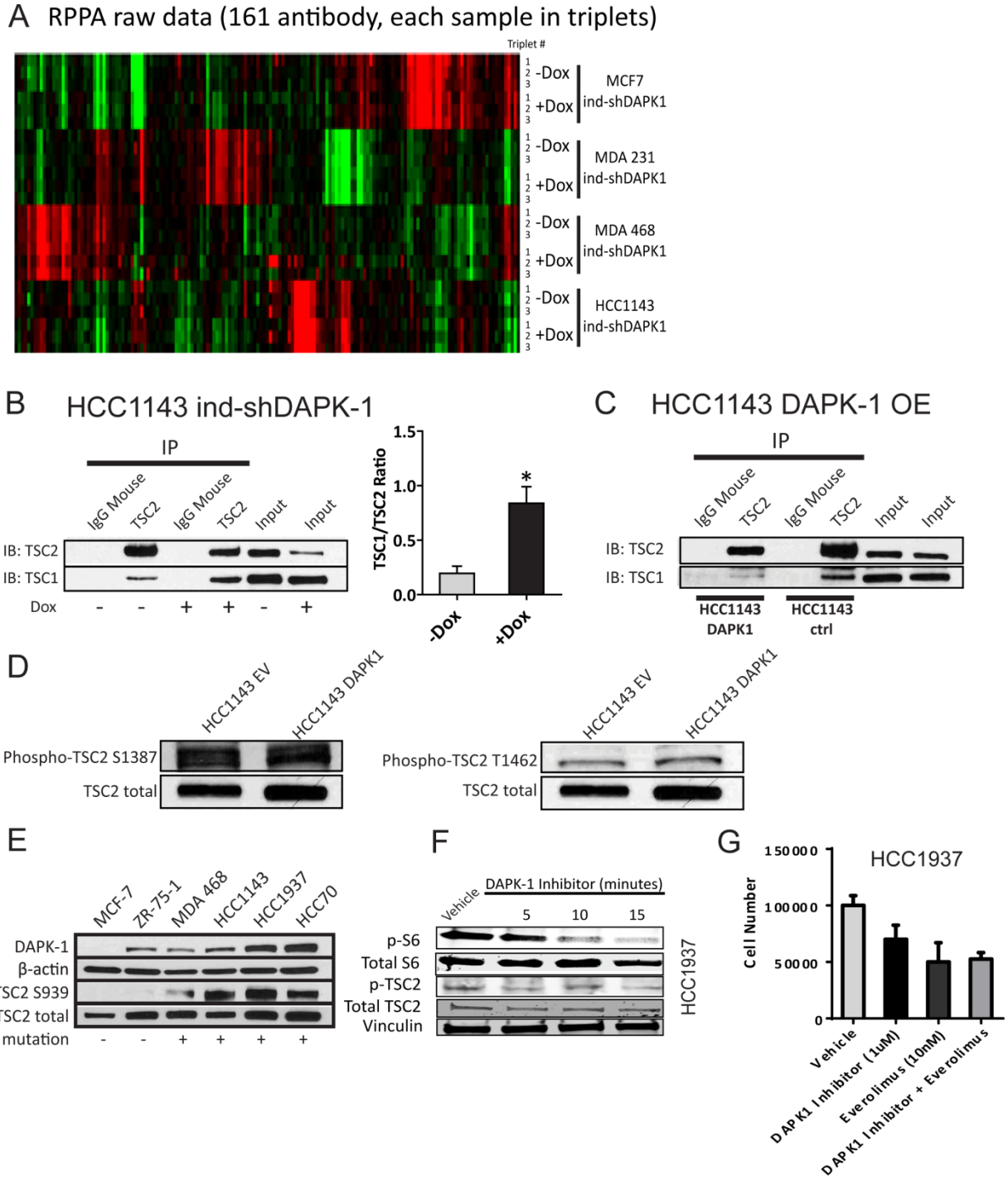

SF4: Co-IP of TSC1/TSC2 complex using TSC2 antibody demonstrates that DAPK1 can modulate TSC1/TSC2 complex formation. A) Raw data of RPPA. **B**) Co-IP of TSC1/TSC2 complex using TSC2 antibody in HCC1143 before and after DAPK1 knockdown. Western blots of IP are shown in the **Left Panel**, the quantification of protein level is shown in the **Right Panel**. **C)** Co-IP of TSC1/TSC2 complex using TSC2 antibody in HCC1143 control and HCC1143 DAPK1 overexpression cell lines **D)** Western blots of p-TSC2 at Ser 1387, Thr1462 and total TSC2 in HCC1143 control and DAPK1 overexpression cells. **E)** Western blots for the indicated proteins across the breast cancer cell lines used in this study. Mutational status of *TP53* is annotated for each cell line. **F)** Immunoblots for activated DAPK1 signaling in HCC1937 cells over a timecourse following DAPK1 inhibitor treatment (1 μM). **G)** Cell viability assays in HCC1937 cells after 6 days of treatment with Everolimus and the DAPK1 inhibitor alone or in combination. Each data was performed in triplicate, with results reported as average ± SEM. *indicates $p<0.01$ and **indicates $p<0.001$ by 2-tailed Student's *t* test.

FIGURE S5, related to Figure 7

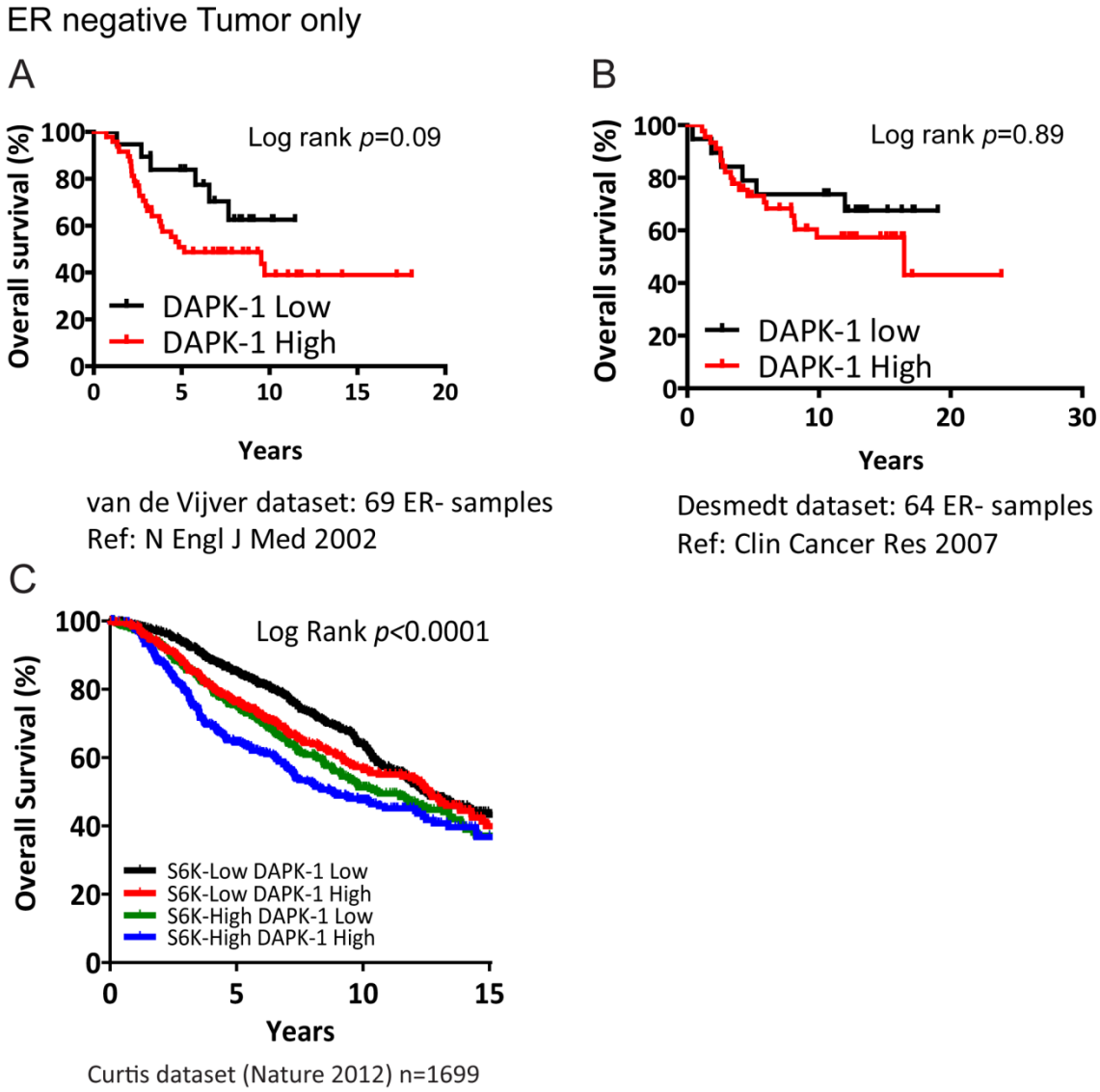

SF5: Patients with high DAPK1 expression are associated with worse clinical outcome in ER-negative breast tumors. A) Kaplan-Meier curves of overall survival in patients with ER-negative tumors from the van de Vijver dataset (2). **B)** Kaplan-Meier curves of overall survival in patients with ER-negative tumors from the Desmedt dataset (1). **C)** Kaplan-Meier curves of overall survival as a function of the combination of S6Kinase expression and DAPK1 expression in the Curtis dataset. For overall survival analysis, log-rank (Mantel-Cox) test was used to determine the statistical difference between stratified groups, A value of $p<0.05$ was considered statistically significant.

FIGURE S6

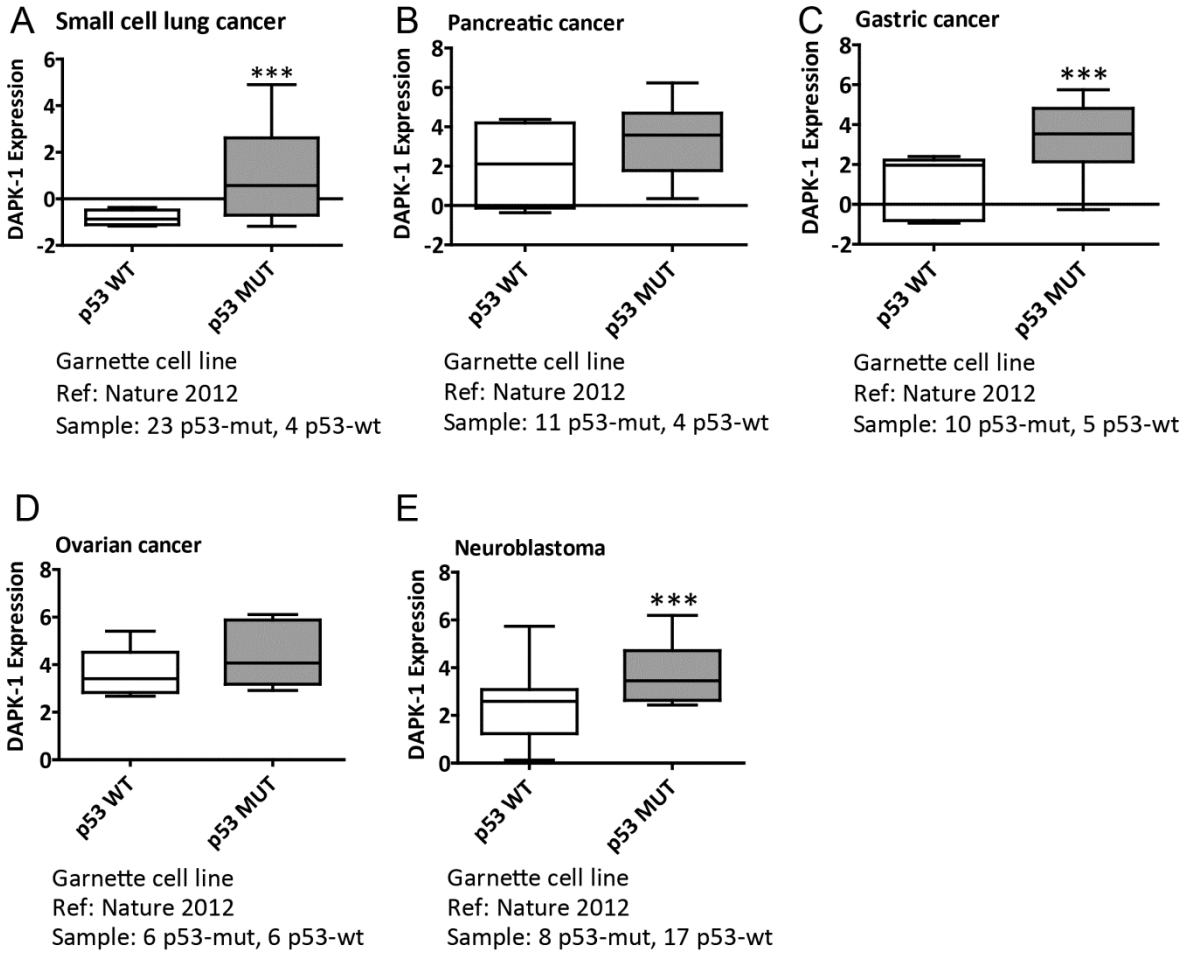

SF6: DAPK1 expression is elevated in p53-mutant tumors compared to p53-wildtype tumors in multiple cancer types. A) Expression of DAPK1 in p53-mutant and p53-wildtype small cell lung cancer cell lines from Garnette dataset (7). **B)** Expression of DAPK1 in p53-mutant and p53-wildtype pancreatic cancer cell lines from Garnette dataset (7). **C)** Expression of DAPK1 in p53-mutant and p53-wildtype gastric cancer cell lines from Garnette dataset (7). **D)** Expression of DAPK1 in p53-mutant and p53-wildtype ovarian cancer cell lines from Garnette dataset (7). **E)** Expression of DAPK1 in p53-mutant and p53-wildtype neuroblastoma lines from Garnette dataset (7). Two-tailed Student's *t* test was used for statistical analysis**.** ***indicates $p<0.0001$.

Table S1: shRNA Oligonucleotide ID

ShRNA	Description	Item	Clone ID
DAPK1 shRNA #1	pGIPZ lentiviral shRNAmir clone	RHS4430-100987091	V3LHS_413770
DAPK1 shRNA #2	pGIPZ lentiviral shRNAmir clone	RHS4430-99881952	V3LHS_643942
P53 shRNA	pGIPZ lentiviral shRNAmir clone	RHS4430-98486236	V2LHS_217

Table S1: List of shRNA Oligonucleotide ID. shRNA used in this study was obtained from Openbiosystems (Huntsville, AL). The clone ID and catalog number are listed in the table.

Table S2: siRNA Oligonucleotide ID

Target gene	Oligo#	Name	Sequence
DAPK1	1278391	SASI_Hs01_00238225	GAGAAUCGAUGUCCAGGAU[dT][dT]
	1278392	SASI_Hs01_00238225_AS	AUCCUGGACAUCGAUUCUC[dT][dT]
DAPK1	1278387	SASI_Hs01_00238226	CAACUAUGAUGUUAACCAA[dT][dT]
	1278388	SASI_Hs01_00238226_AS	UUGGUUAACAUCAUAGUUG[dT][dT]
DAPK1	1278389	SASI_Hs01_00238228	GACAUGAAGGUACUUCGAA[dT][dT]
	1278388	SASI_Hs01_00238228_AS	UUCGAAGUACCUUCAUGUC[dT][dT]

Table S2: List of siRNA Oligonucleotide ID. siRNA against DAPK1 used in this study was obtained from Sigma-Aldrich (St. Louis, MO). The Oligo ID and sequences are listed in the table.

Table S3: q-RT-PCR primers and probes

Cyclophilin	F	Human	ACGGCGAGCCCTTGG
	R	Human	TTTCTGCTGTCTTTGGGACCT
	P	Human	CGCGTCTCCTTTGAGCTGTTTGCA
p53	F	Human	ACACGCTTCCCTGGATTG
	R	Human	GATCTGACTGCGGCTCCT
	#8UPL	Human	Roche Universal Probe Library
DAPK1	F	Human	AGGACCTCAGGCGCATTG
	R	Human	CTGAACTGTTTCACTTTGCATGATG
	P	Human	CAGCTCCACAGCACAGGCGAGATC

Table S3: q-RT-PCR primers and probes. TaqMan assay of cyclophilin and DAPK1 were designed by Primer Express Software V2.0. Primers and probe sequences are listed in the table. Probe for p53 quantification were obtained from Universal Probe Library (#04869877001) from Roche Applied Science (Indianapolis, IN)

Table S4: Fold change of 161 proteins upon DAPK1 knockdown

Protein Name	MCF7	HCC1143
14-3-3_epsilon-M-C	0.97	0.94
4E-BP1-R-V	1.11	1.16
4E-BP1_pS65-R-V	1.15	0.75
4E-BP1_pT70-R-C	1.03	0.92
4EBP1_pT37-T46-R-V	1.21	0.99
53BP1-R-C	0.92	0.89
ACC_pS79-R-V	1.42	1.19
ACC1-R-C	0.88	0.78
AIB1-M-V	1.06	1.04
Akt-R-V	0.80	0.97
Akt_pS473-R-V	2.09	1.39
Akt_pT308-R-V	0.83	1.02
alpha-Catenin-M-V	1.17	1.11
AMPK_alpha-R-C	1.01	1.07
AMPK_pT172-R-V	1.29	1.53
Annexin_I-R-V	1.42	0.96
AR-R-V	1.22	1.14
Bak-R-C	1.08	0.89
Bax-R-V	0.91	0.94
Bcl-2-M-V	0.57	1.12
Bcl-2-R-C	0.51	0.99
Bcl-X-R-C	0.98	0.95
Bcl-xL-R-V	0.90	1.02
Beclin-G-V	0.98	1.13
beta-Catenin-R-V	0.78	1.29
Bid-R-C	0.99	0.96
Bim-R-V	1.22	1.30
BRAF-R-NA	0.90	0.96
c-Jun_pS73-R-C	0.81	0.56
c-Kit-R-V	0.96	0.69
c-Met-M-C	1.01	2.30
c-Met_pY1235-R-C	1.00	0.98
c-Myc-R-C	0.70	0.61
C-Raf-R-V	0.90	0.82
C-Raf_pS338-R-C	1.07	0.97
Caspase-3_active-R-C	0.99	0.98

Caspase-7_cleavedD198-R-C	1.17	1.00
Caspase-9_cleavedD330-R-C	0.76	0.80
Caveolin-1-R-V	1.02	0.58
CD31-M-V	1.10	0.97
CDK1-R-V	0.71	0.63
CDK4-M-C	0.93	0.74
Chk1_pS345-R-C	1.24	0.96
Chk2-M-C	0.78	1.03
Chk2_pT68-R-C	1.01	0.87
cIAP-R-V	1.13	1.01
Claudin-7-R-V	0.91	1.76
Collagen_VI-R-V	1.84	1.06
COX-2-R-C	0.63	0.82
Cyclin_B1-R-V	0.76	0.60
Cyclin_D1-R-V	1.07	0.90
Cyclin_E1-M-V	1.15	0.88
DJ-1-R-C	0.90	1.00
Dvl3-R-V	0.95	1.06
E-Cadherin-R-V	0.86	1.24
eEF2-R-V	0.70	0.86
eEF2K-R-V	0.96	0.75
EGFR-R-C	1.04	1.00
EGFR_pY1068-R-V	1.06	1.44
EGFR_pY1173-R-C	1.09	1.08
EGFR_pY992-R-V	1.09	1.10
eIF4E-R-V	1.06	1.07
ER-alpha-R-V	0.52	1.32
ER-alpha_pS118-R-V	0.89	1.09
ERCC1-M-C	0.85	1.51
FAK-R-C	1.01	0.99
Fibronectin-R-C	1.10	0.32
FOXO3a-R-C	1.00	1.08
FOXO3a_pS318_S321-R-C	1.08	1.42
GAB2-R-V	1.10	1.25
GATA3-M-V	0.76	1.12
GSK3-alpha-beta-M-V	1.06	0.99
GSK3-alpha-beta_pS21_S9-R-V	1.33	1.30
GSK3_pS9-R-V	1.60	1.30
HER2-M-V	0.95	0.96
HER2_pY1248-R-V	0.95	1.10
HER3-R-V	1.16	1.01
HER3_pY1298-R-C	1.07	1.05
HSP70-R-C	0.91	0.94

IGF-1R-beta-R-C	0.81	0.97
IGFBP2-R-V	0.72	1.02
INPP4B-G-C	0.80	0.99
IRS1-R-V	0.77	0.81
JNK_ pT183-T185-R-C	0.94	0.85
JNK2-R-C	0.93	0.95
K-Ras-M-C	1.07	1.11
MAPK_pT202_Y204-R-V	0.88	0.92
Mcl1-M-C	1.02	1.09
MEK1-R-V	0.80	0.99
MEK1_pS217_S221-R-V	0.91	1.05
MIG-6-M-V	1.05	0.93
Mre11-R-C	1.05	1.03
MSH2-M-C	0.97	0.86
MSH6-R-C	0.66	0.75
mTOR-R-V	0.86	1.27
mTOR_ pS2448-R-C	1.31	1.08
N-Cadherin-R-V	0.86	0.99
NF-kB-p65_pS536-R-C	1.02	0.58
NF2-R-C	0.71	0.69
Notch1-R-V	0.94	0.89
Notch3-R-C	1.21	1.11
P-Cadherin-R-C	0.96	1.14
p21-R-C	0.82	0.84
p27-R-V	1.09	0.89
p27_pT157-R-C	0.94	0.99
p27_pT198-R-V	1.09	1.03
p38_MAPK-R-C	1.02	0.88
p38_pT180_Y182-R-V	0.94	0.81
p53-R-V	1.08	0.79
p70S6K-R-V	1.01	0.96
p70S6K_pT389-R-V	1.53	0.44
p90RSK_pT359_S363-R-C	1.01	0.91
PARP_cleaved-M-C	1.14	2.49
Paxillin-R-V	0.99	1.12
PCNA-M-V	0.69	0.55
PDK1_pS241-R-V	1.18	1.03
PI3K-p110-alpha-R-C	1.01	1.00
PI3K-p85-R-V	0.88	1.00
PKC-alpha-M-V	0.89	1.07
PKC-alpha_pS657-R-V	1.11	1.19
PR-R-V	0.82	0.96
PRAS40_pT246-R-V	1.48	0.86

PTCH-R-C	0.90	1.41
PTEN-R-V	0.94	1.07
Rab11-R-V	1.07	1.02
Rab25-R-C	1.03	1.81
Rad50-M-C	0.92	1.07
Rad51-M-C	0.90	0.93
Rb-M-V	0.82	1.85
Rb_pS807_S811-R-V	0.52	0.45
S6_pS235_S236-R-V	1.04	0.27
S6_pS240_S244-R-V	1.12	0.30
Smac-M-V	1.20	1.02
Smad1-R-V	1.10	1.04
Smad3-R-V	1.07	1.15
Smad4-M-V	1.03	1.07
Smad5 pS463_S465-R-C	1.25	0.84
Snail-M-C	0.96	2.22
Src-M-V	1.00	1.15
SRC-R-C	0.85	1.28
Src_pY416-R-C	0.90	0.97
Src_pY527-R-V	0.88	1.13
STAT3_pY705-R-V	0.82	1.00
STAT5-alpha-R-V	0.89	0.85
Stathmin-R-V	0.95	0.85
Survivin-M-C	0.99	2.71
Syk-M-V	0.99	0.84
Tau-M-C	0.90	1.08
TAZ_pS89-R-C	1.06	1.02
TIGAR-R-V	1.10	1.44
TTF1-R-V	0.89	0.94
Tuberin-R-C	1.03	0.86
VASP-R-C	1.16	1.14
VEGFR2-R-V	0.82	1.28
XIAP-R-C	1.00	1.12
XRCC1-R-C	0.99	0.99
YAP-R-V	0.92	1.14
YAP_pS127-R-C	1.26	1.18
YB-1-R-V	0.88	1.14
YB-1_pS102-R-V	0.90	0.82
Chk1-R-C	1.00	0.95

Table S4: RPPA analysis of fold changes of 161 proteins after DAPK1 knockdown in MCF7 and HCC1143 cells.

Table S5**:** Proteins differentially regulated in p53-wt MCF7 cells and p53-mut HCC1143 cells are listed.

Differentially regulated proteins Between p53-wt and p53-mut cancer cells	**Fold change**
S6 pS235/236	0.27
S6 pS240/244	0.29
p70S6KpT398	0.44
NF-κB p65 pS536	0.58
CDK4	0.74
4E-BP1 pS65	0.75

Table S5: Listed are the proteins that were significantly changed upon DAPK1 depletion in p53-mutant HCC1143 cells but not changed (or inversely changed) in p53-wildtype MCF7 cells.

Supplementary References

1. Desmedt C, Piette F, Loi S, Wang Y, Lallemand F, Haibe-Kains B, Viale G, Delorenzi M, Zhang Y, d'Assignies MS, et al. Strong time dependence of the 76-gene prognostic signature for node-negative breast cancer patients in the TRANSBIG multicenter independent validation series. *Clinical cancer research : an official journal of the American Association for Cancer Research.* 2007;13(11):3207-14.

2. van de Vijver MJ, He YD, van't Veer LJ, Dai H, Hart AA, Voskuil DW, Schreiber GJ, Peterse JL, Roberts C, Marton MJ, et al. A gene-expression signature as a predictor of survival in breast cancer. *The New England journal of medicine.* 2002;347(25):1999-2009.

3. Karnoub AE, Dash AB, Vo AP, Sullivan A, Brooks MW, Bell GW, Richardson AL, Polyak K, Tubo R, and Weinberg RA. Mesenchymal stem cells within tumour stroma promote breast cancer metastasis. *Nature.* 2007;449(7162):557-63.

4. Gao J, Aksoy BA, Dogrusoz U, Dresdner G, Gross B, Sumer SO, Sun Y, Jacobsen A, Sinha R, Larsson E, et al. Integrative analysis of complex cancer genomics and clinical profiles using the cBioPortal. *Science signaling.* 2013;6(269):pl1.

5. Cerami E, Gao J, Dogrusoz U, Gross BE, Sumer SO, Aksoy BA, Jacobsen A, Byrne CJ, Heuer ML, Larsson E, et al. The cBio cancer genomics portal: an open platform for exploring multidimensional cancer genomics data. *Cancer discovery.* 2012;2(5):401-4.

6. Curtis C, Shah SP, Chin SF, Turashvili G, Rueda OM, Dunning MJ, Speed D, Lynch AG, Samarajiwa S, Yuan Y, et al. The genomic and transcriptomic architecture of 2,000 breast tumours reveals novel subgroups. *Nature.* 2012;486(7403):346-52.

7. Garnett MJ, Edelman EJ, Heidorn SJ, Greenman CD, Dastur A, Lau KW, Greninger P, Thompson IR, Luo X, Soares J, et al. Systematic identification of genomic markers of drug sensitivity in cancer cells. *Nature.* 2012;483(7391):570-5.

Blots For Main Figures

Figure 1B

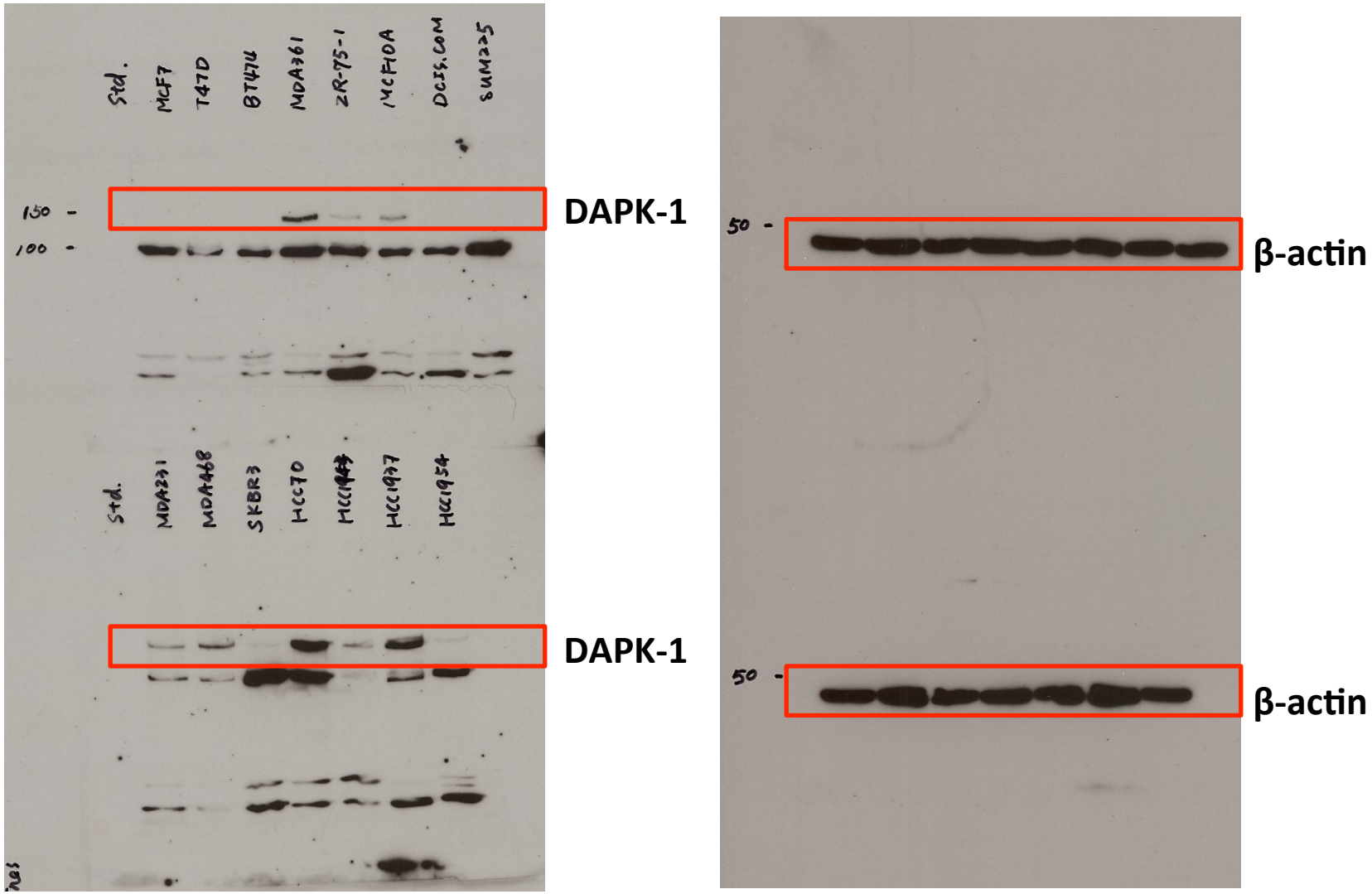
Std.
MCF7
T47D
BT474
MDA361
ZR-75-1
MCF10A
DCIS.COM
SUM225
150
100
DAPK-1
Std.
MDA231
MDA468
SKBR3
HCC70
HCC1937
HCC1954
DAPK-1
50
β-actin
50
β-actin

Figure 3B

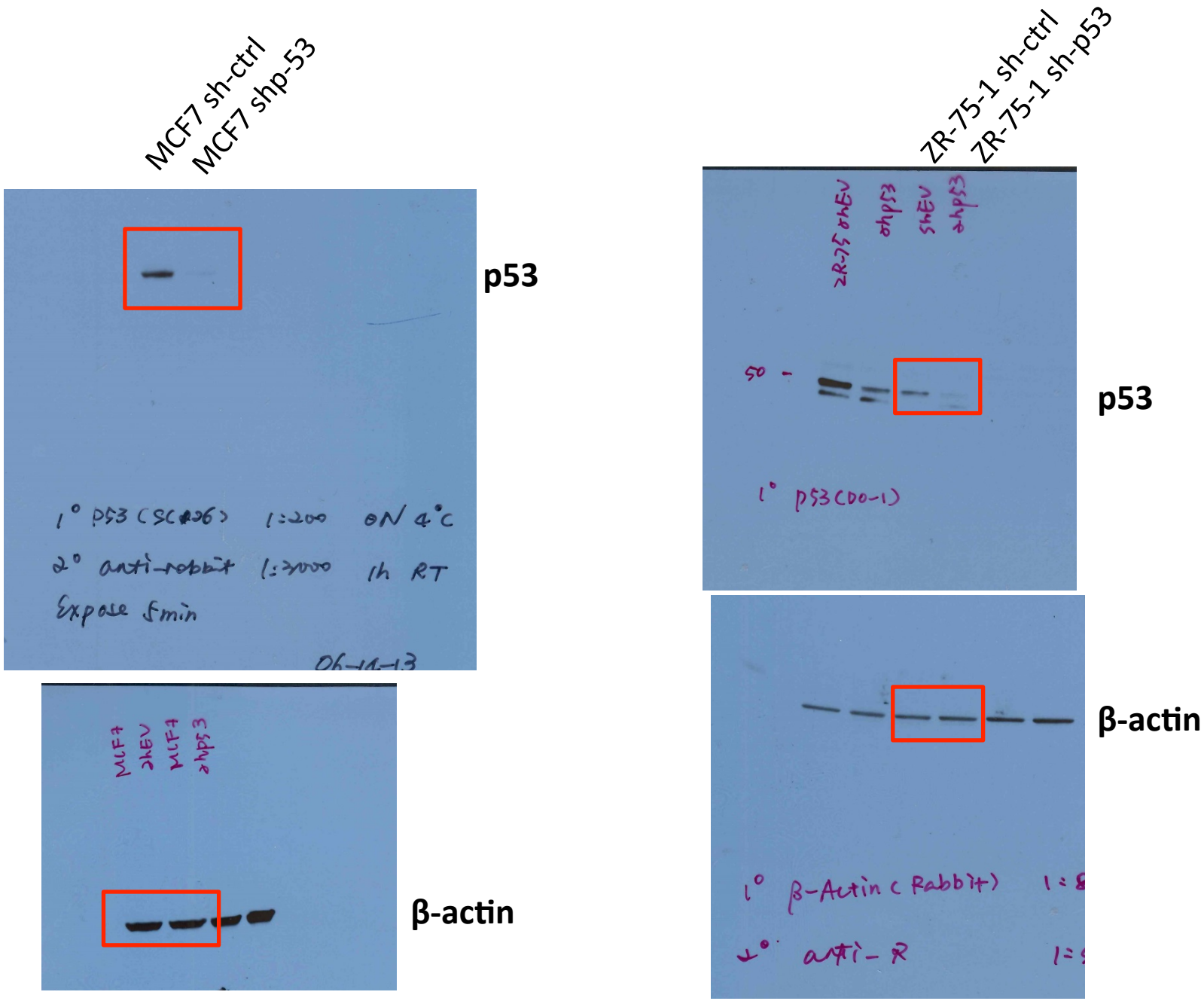
MCF7 sh-ctrl
MCF7 shp-53
p53
1° p53 (SC-126) 1:200 ON 4°C
2° anti-rabbit 1:3000 1h RT
Expose 5min
β-actin
ZR-75-1 sh-ctrl
ZR-75-1 sh-p53
p53
1° p53 (DO-1)
β-actin
1° β-Actin (Rabbit)

Figure 3C

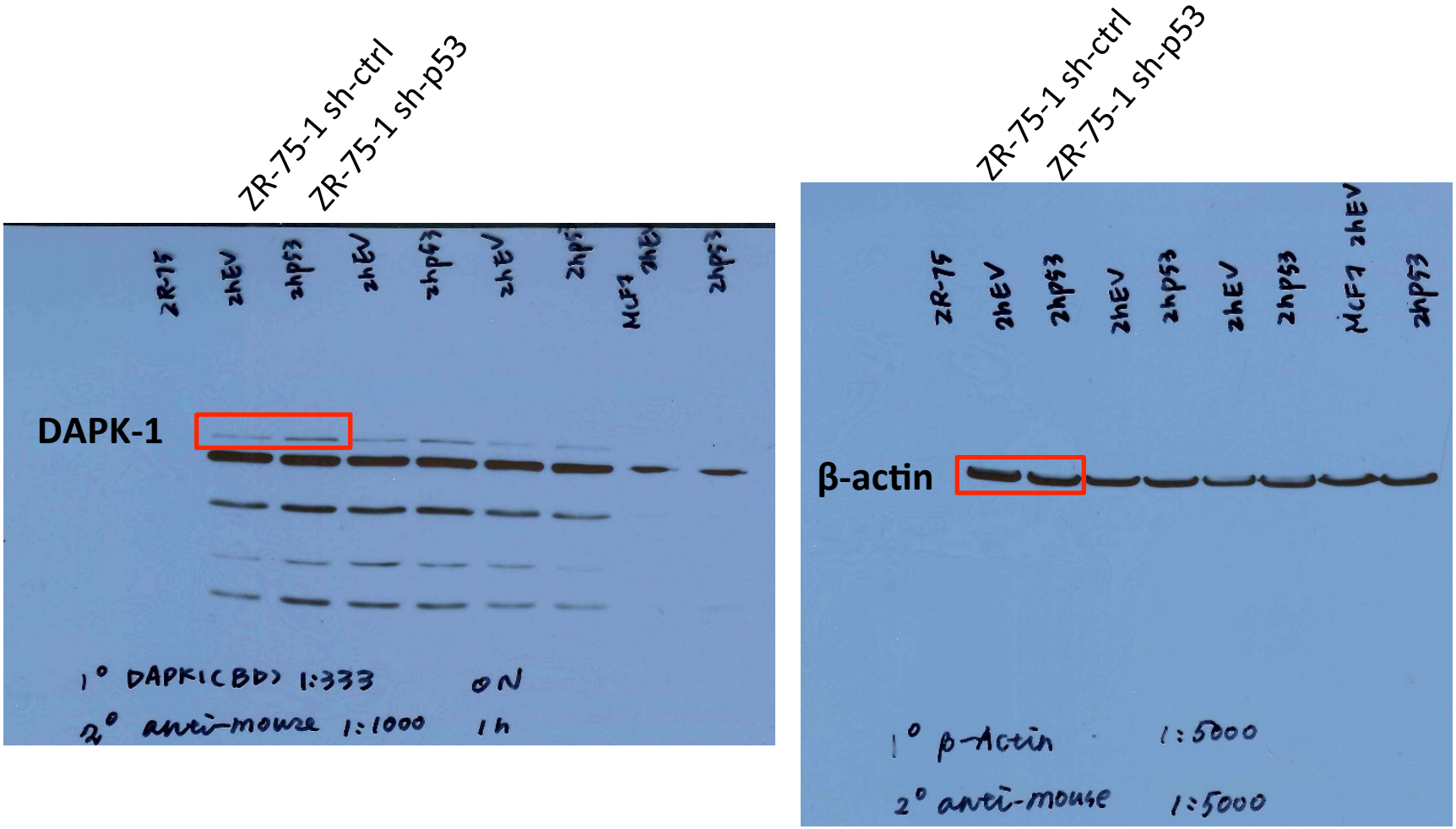
ZR-75-1 sh-ctrl
ZR-75-1 sh-p53
DAPK-1
1° DAPK (CBD) 1:333 ON
2° anti-mouse 1:1000 1h
ZR-75-1 sh-ctrl
ZR-75-1 sh-p53
β-actin
1° β-Actin 1:5000
2° anti-mouse 1:5000

Figure 4A (inserted panel)

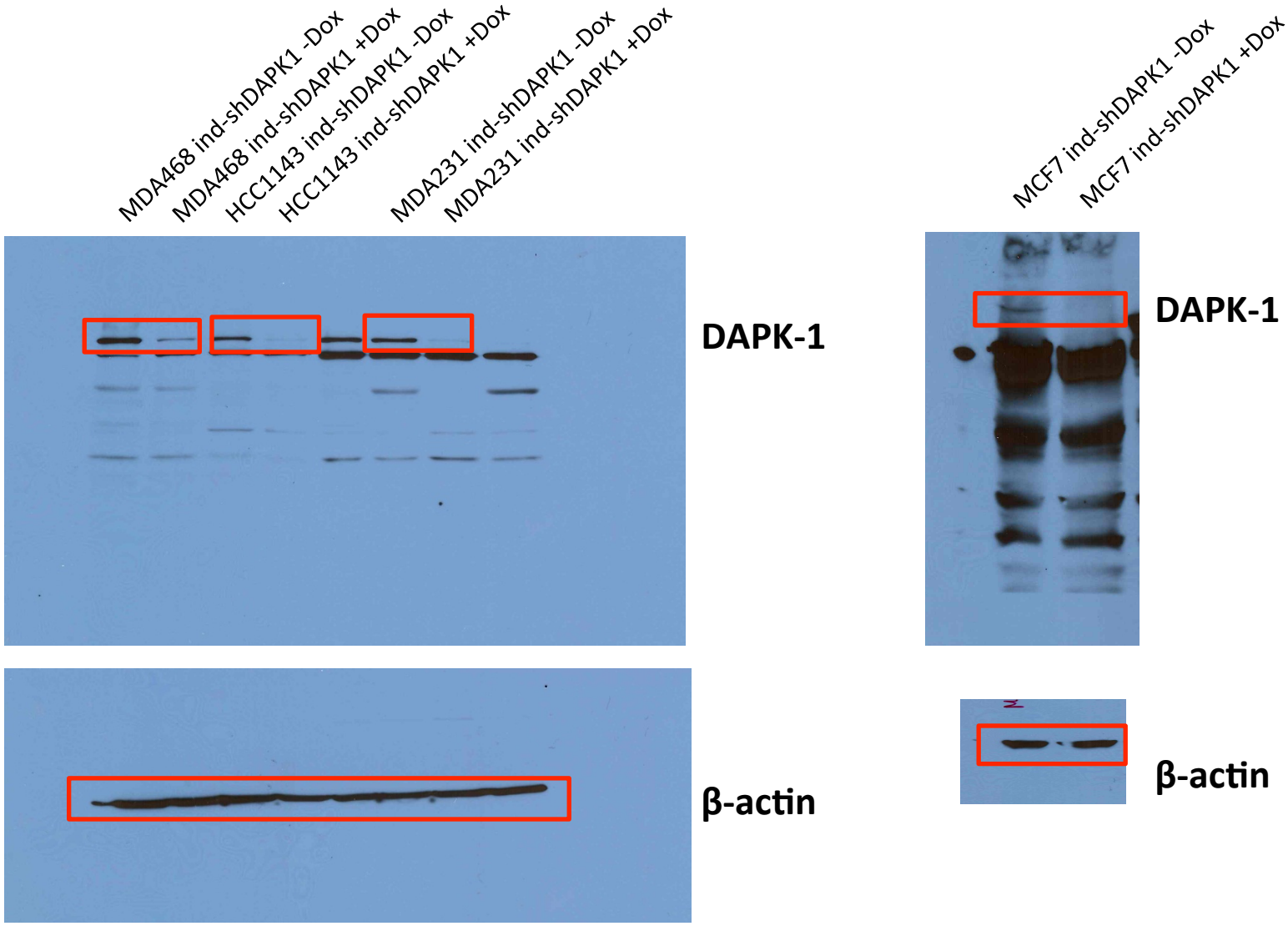

Figure 5F

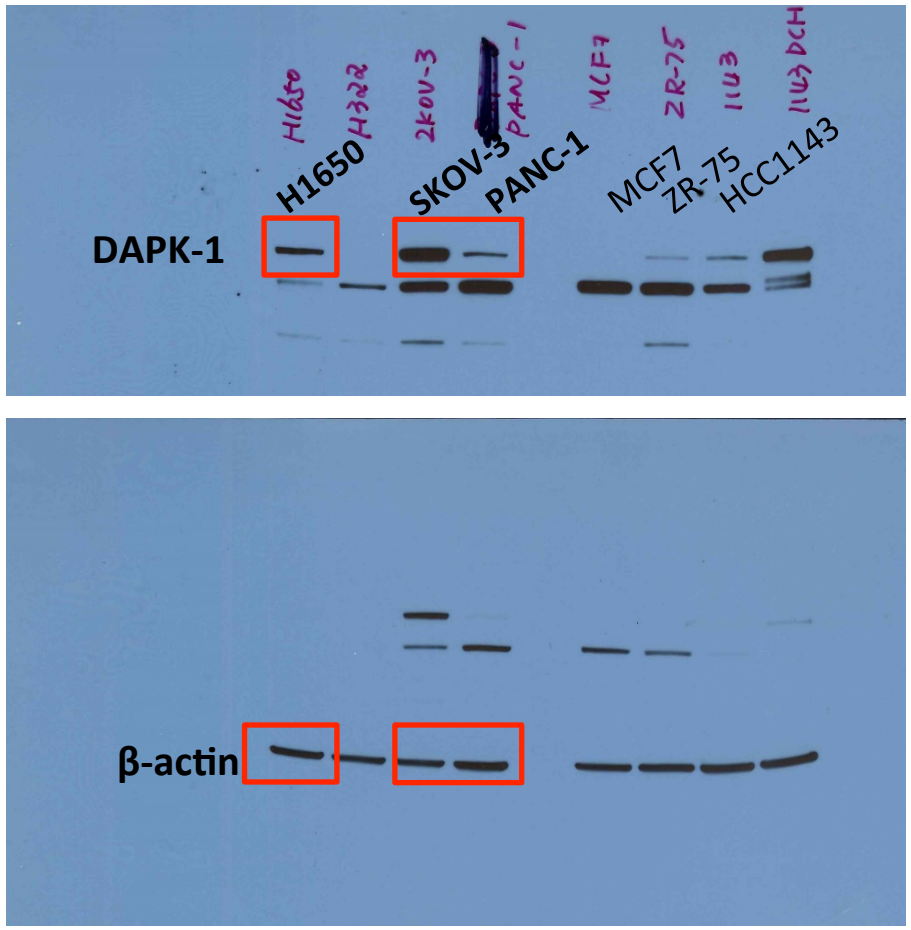

Figure 6B

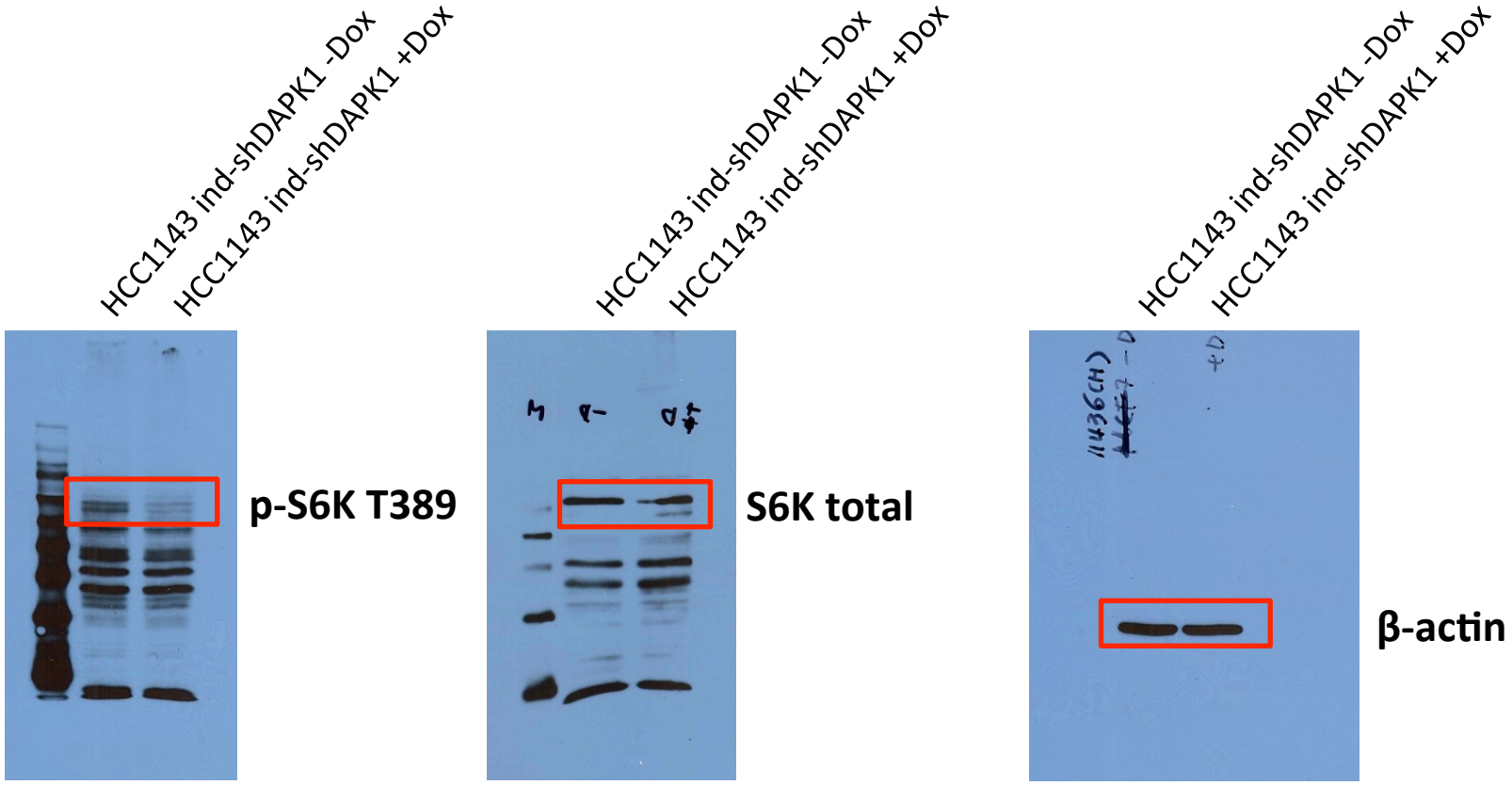
HCC1143 ind-shDAPK1 -Dox
HCC1143 ind-shDAPK1 +Dox
p-S6K T389
HCC1143 ind-shDAPK1 -Dox
HCC1143 ind-shDAPK1 +Dox
S6K total
HCC1143 ind-shDAPK1 -Dox
HCC1143 ind-shDAPK1 +Dox
β-actin

Figure 6B (continued)

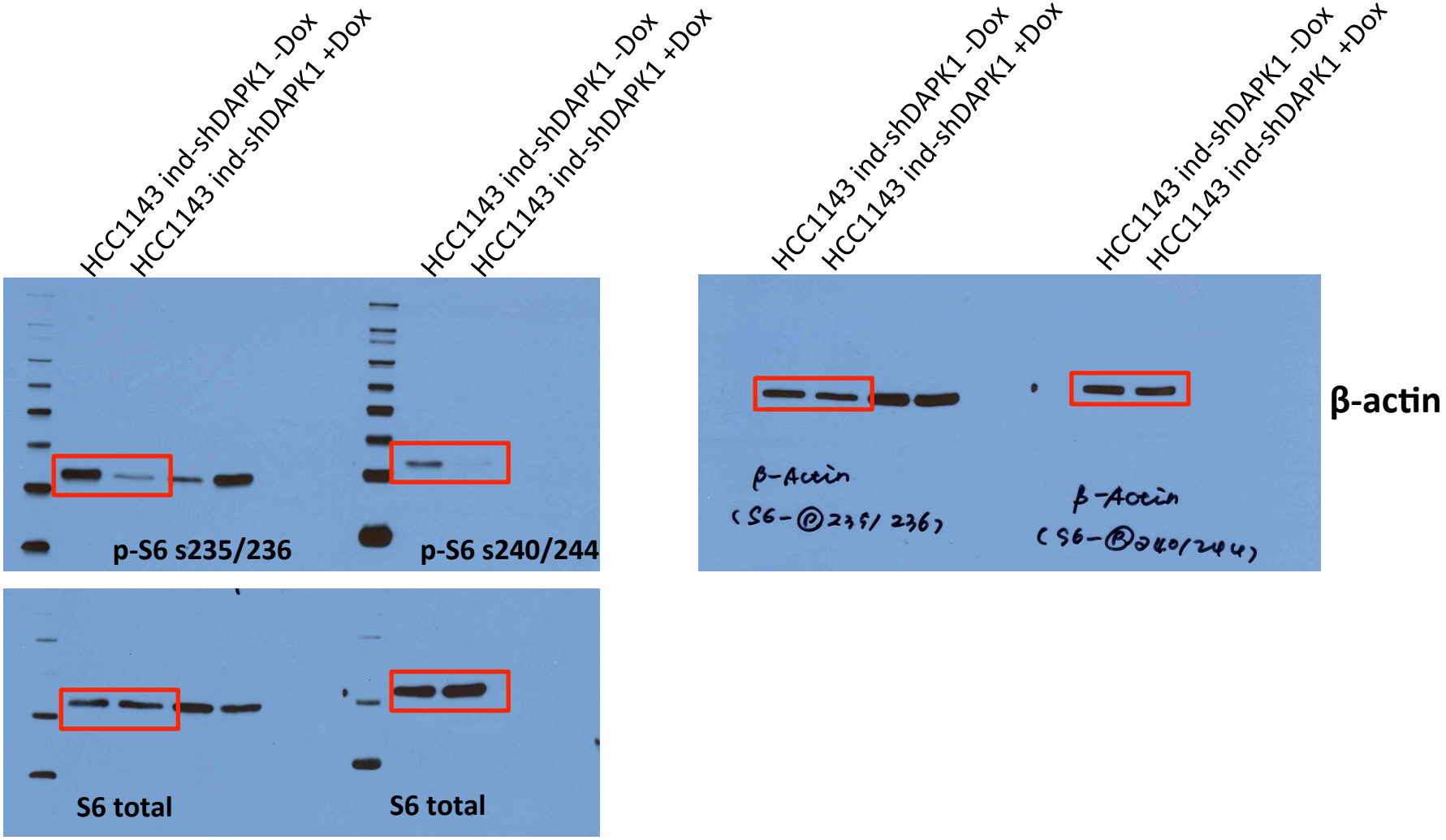

Figure 6C

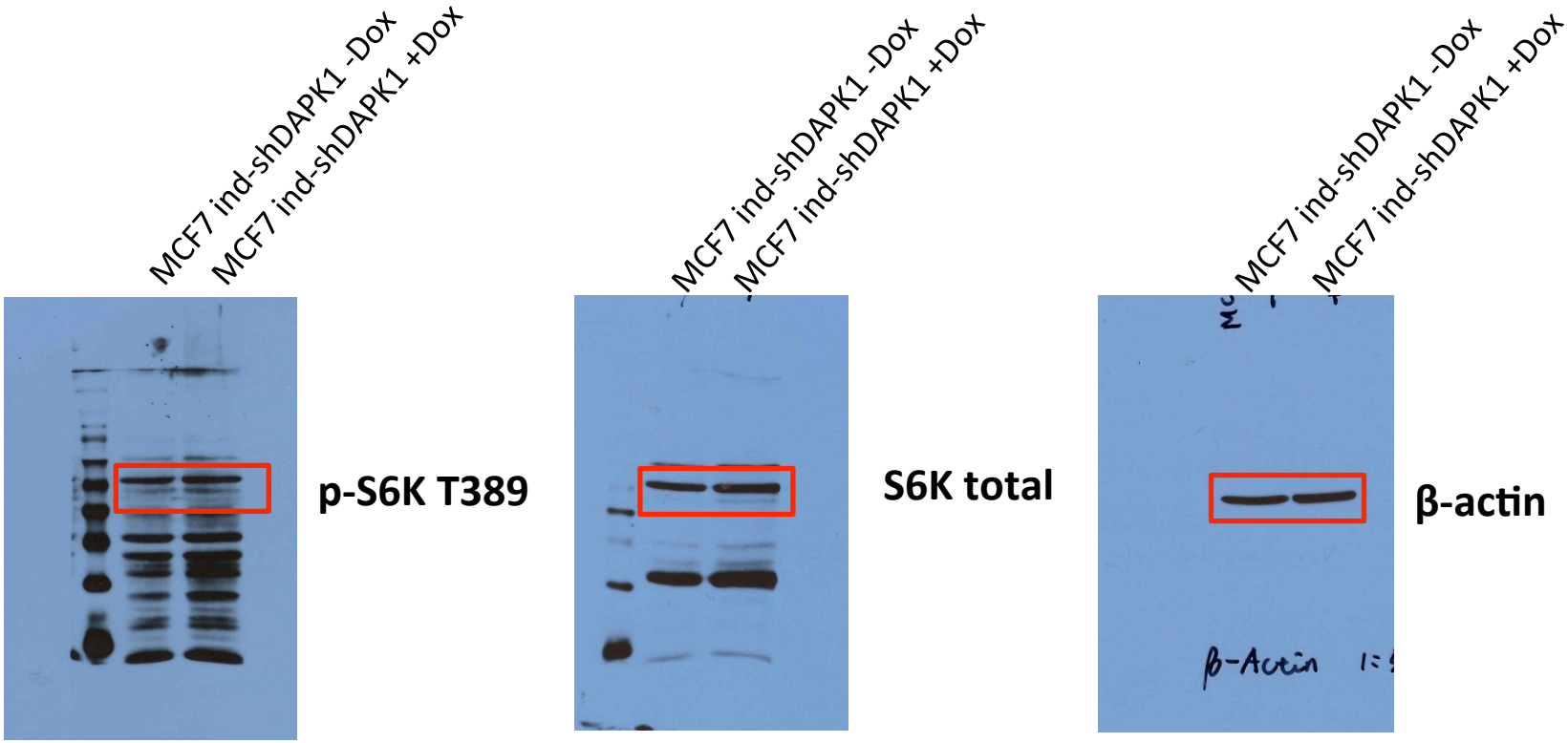
MCF7 ind-shDAPK1 -Dox
MCF7 ind-shDAPK1 +Dox
p-S6K T389
MCF7 ind-shDAPK1 -Dox
MCF7 ind-shDAPK1 +Dox
S6K total
MCF7 ind-shDAPK1 -Dox
MCF7 ind-shDAPK1 +Dox
β-actin
β-Actin

Figure 6C (continued)

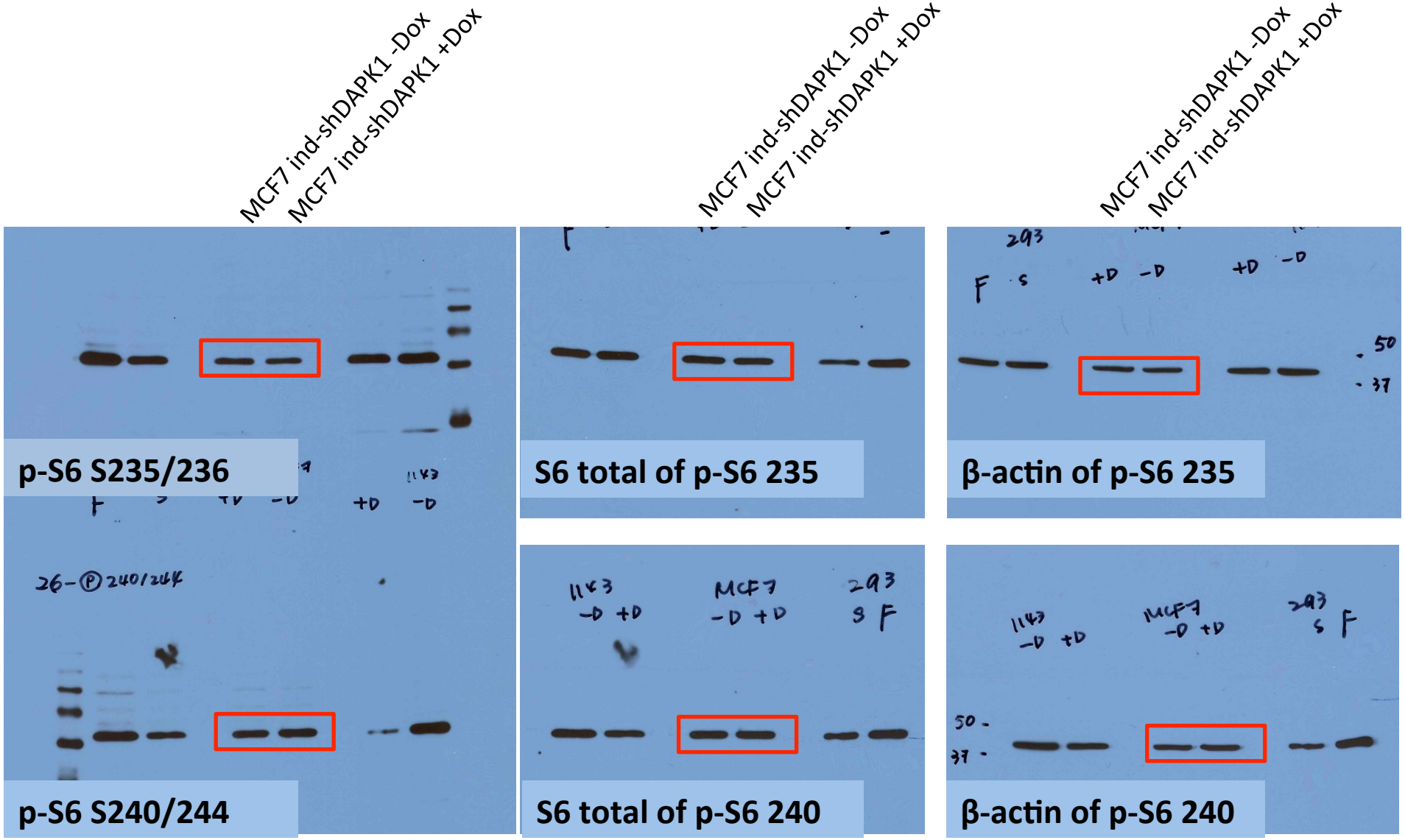

Figure 6D

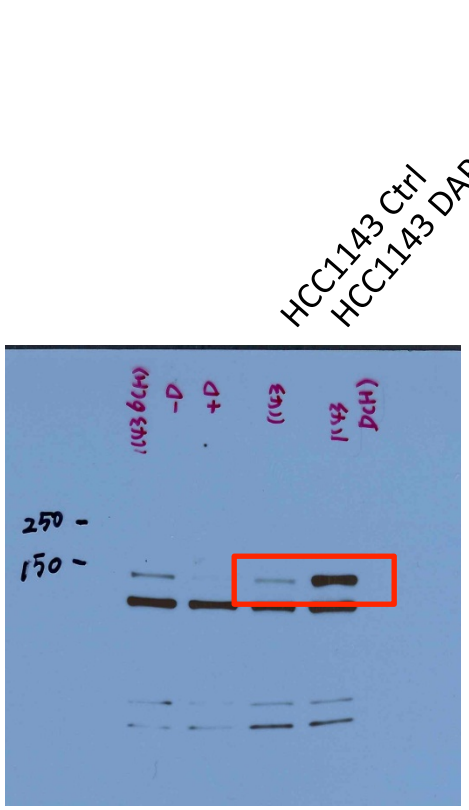

DAPK-1

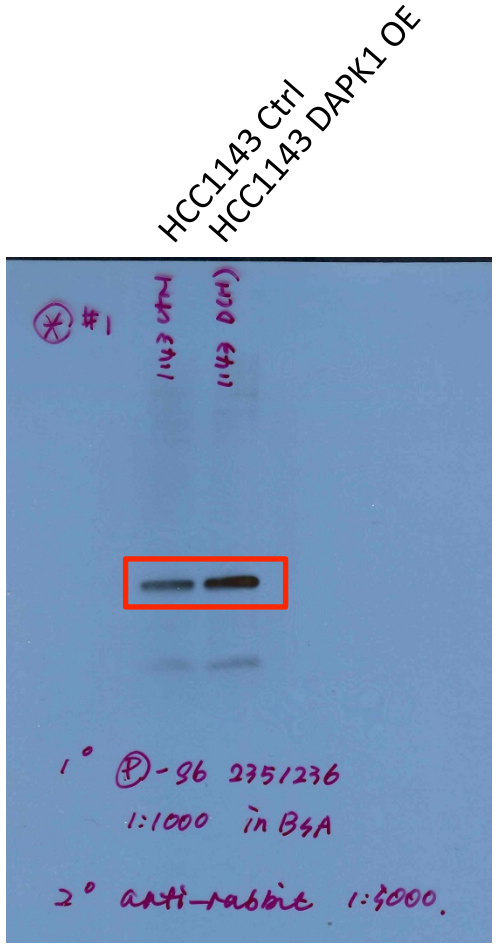

p-S6 S235/236

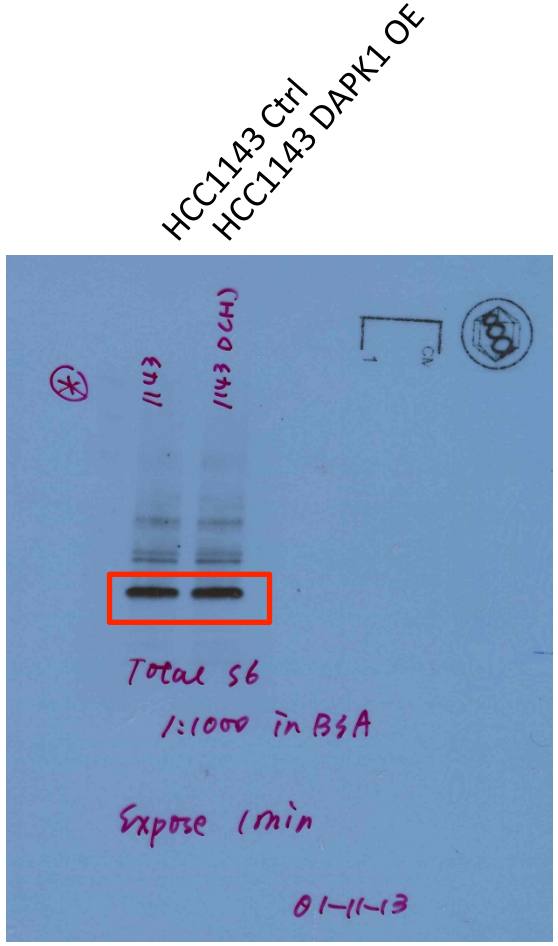

S6 total

Figure 6E

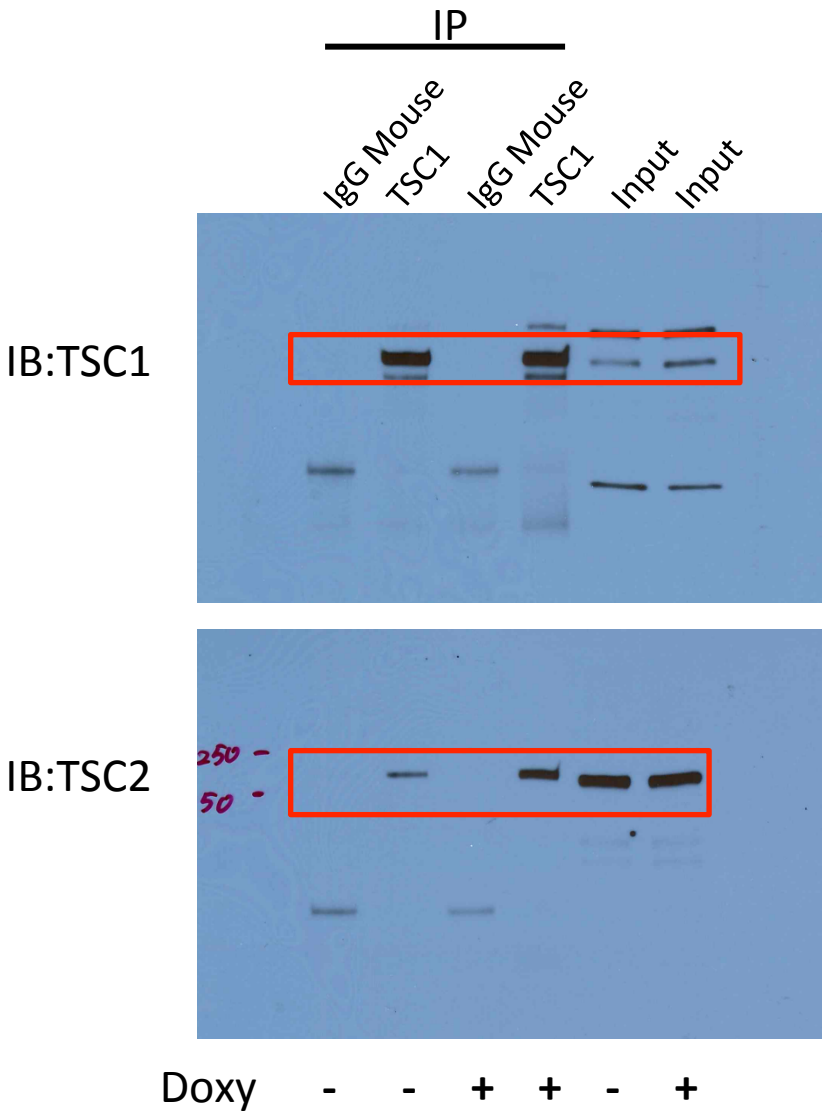
IP
IgG Mouse
TSC1
IgG Mouse
TSC1
Input
Input
IB:TSC1
IB:TSC2
250
50
Doxy - - + + - +

Figure 6F

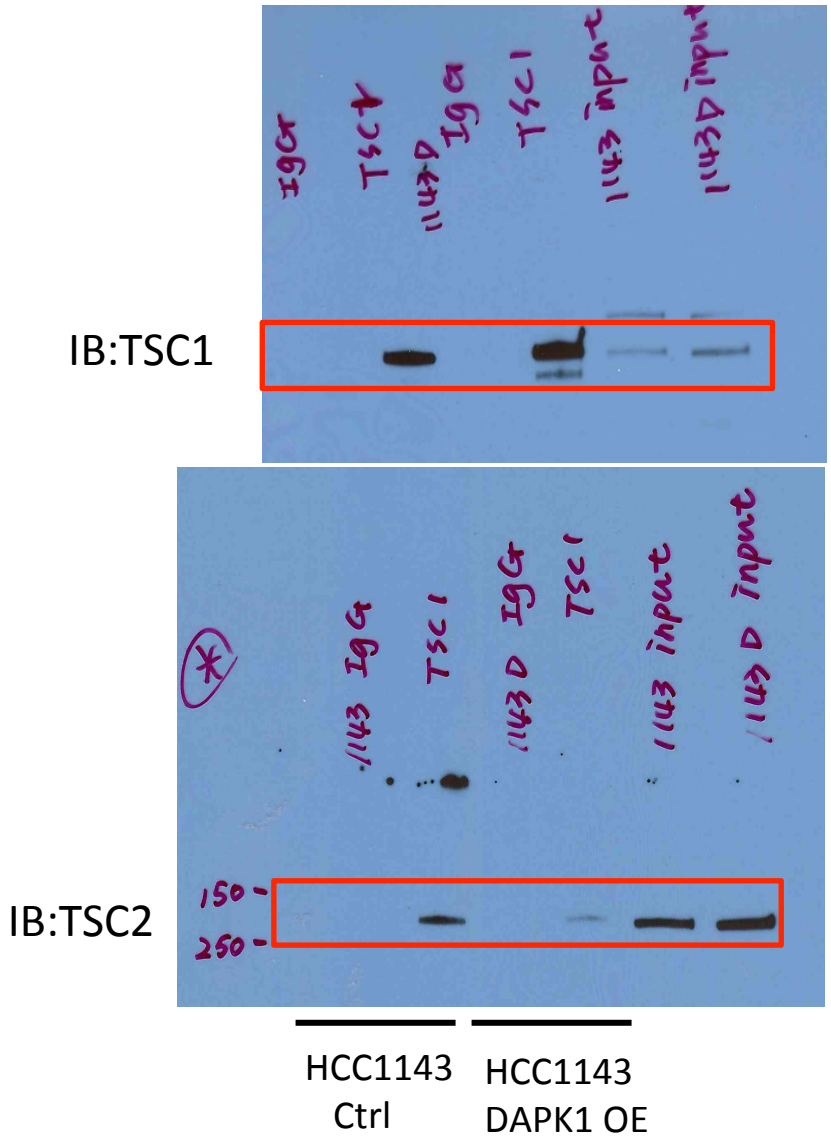
IB:TSC1
IB:TSC2
IgG
TSC1
1143D ctrl
1143 input
1143D input
1143 IgG
TSC1
1143D IgG
TSC1
1143 input
1143D input
150
250
HCC1143
Ctrl
HCC1143
DAPK1 OE

Figure 6G

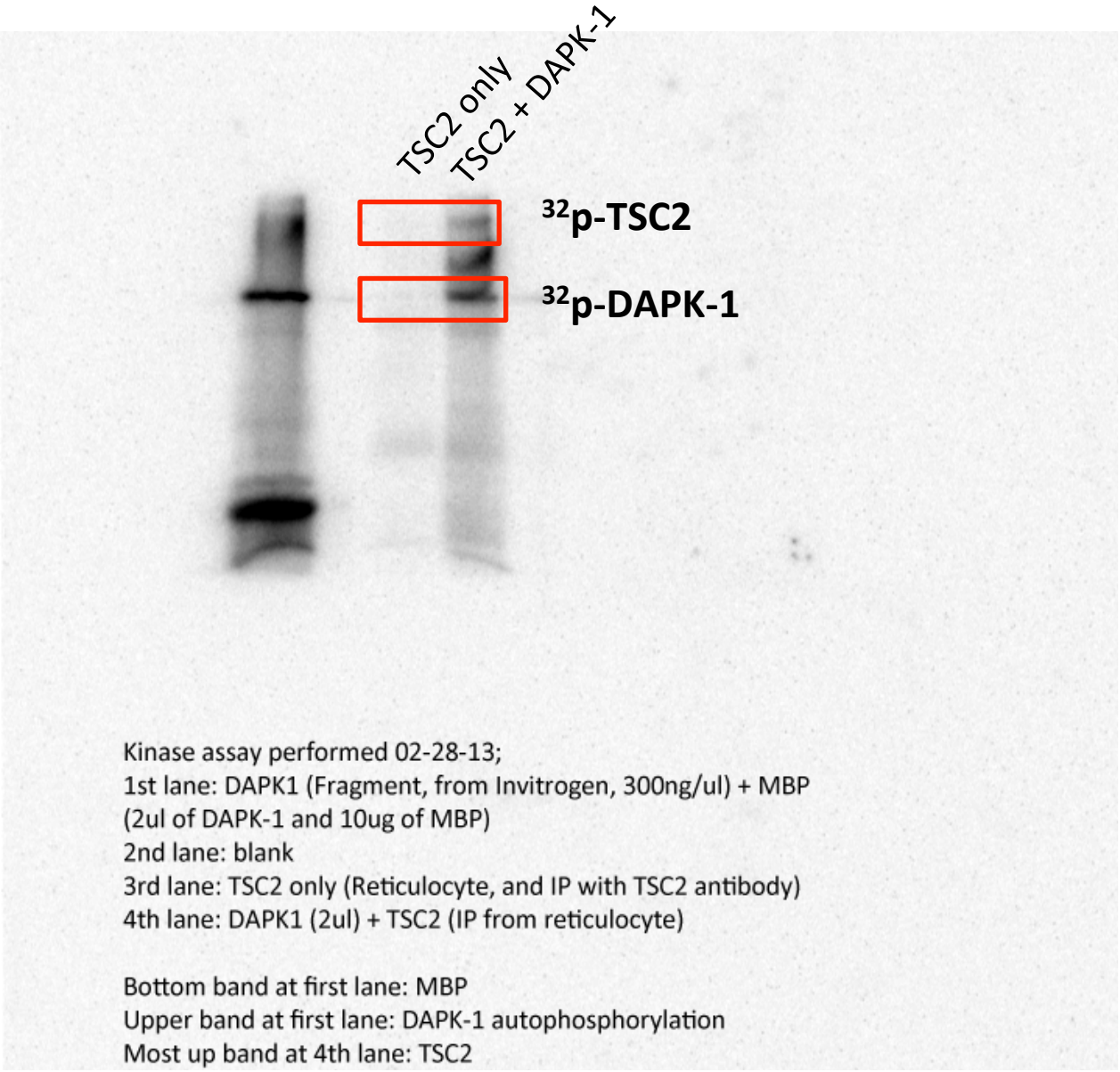
TSC2 only
TSC2 + DAPK-1
32p-TSC2
32p-DAPK-1
Kinase assay performed 02-28-13;
1st lane: DAPK1 (Fragment, from Invitrogen, 300ng/ul) + MBP
(2ul of DAPK-1 and 10ug of MBP)
2nd lane: blank
3rd lane: TSC2 only (Reticulocyte, and IP with TSC2 antibody)
4th lane: DAPK1 (2ul) + TSC2 (IP from reticulocyte)
Bottom band at first lane: MBP
Upper band at first lane: DAPK-1 autophosphorylation
Most up band at 4th lane: TSC2

Figure 6H

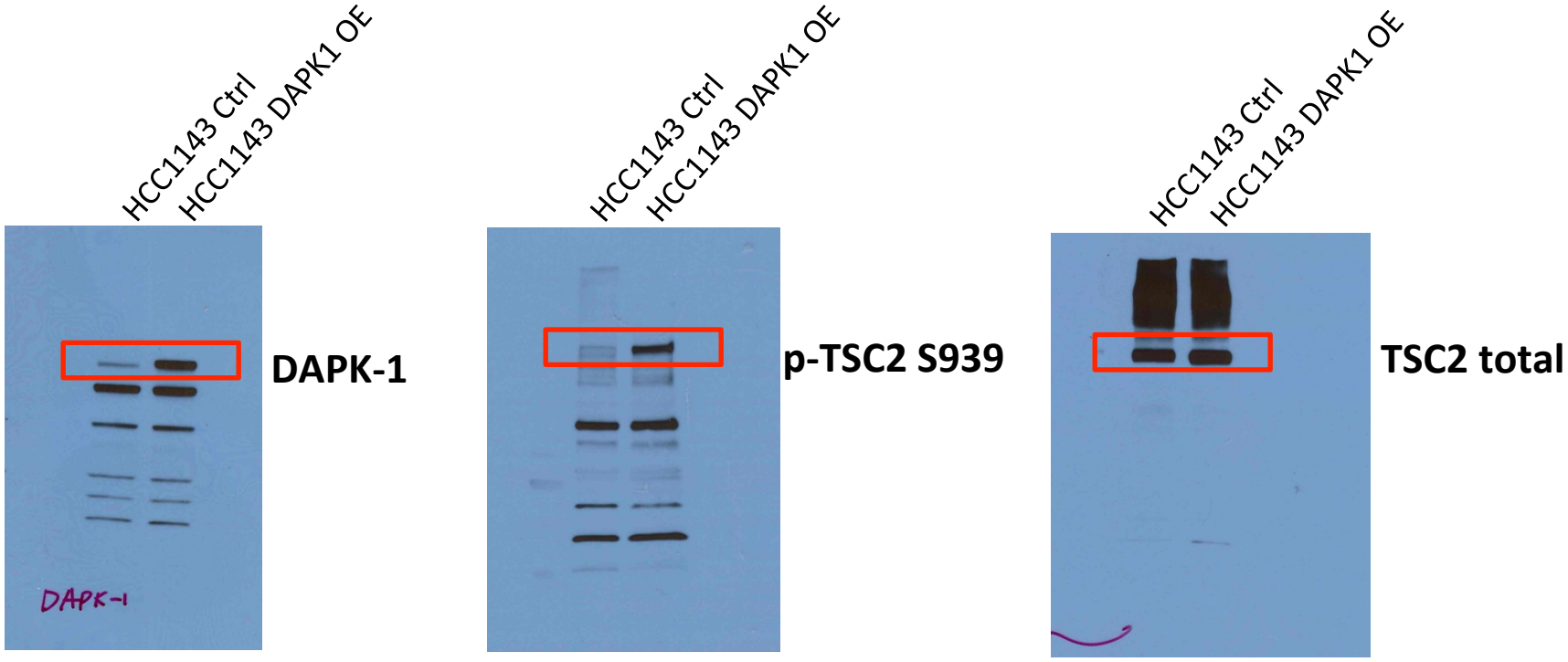
HCC1143 Ctrl
HCC1143 DAPK1 OE
DAPK-1
HCC1143 Ctrl
HCC1143 DAPK1 OE
p-TSC2 S939
HCC1143 Ctrl
HCC1143 DAPK1 OE
TSC2 total

Blots For Supplementary Figures

Figure S1G

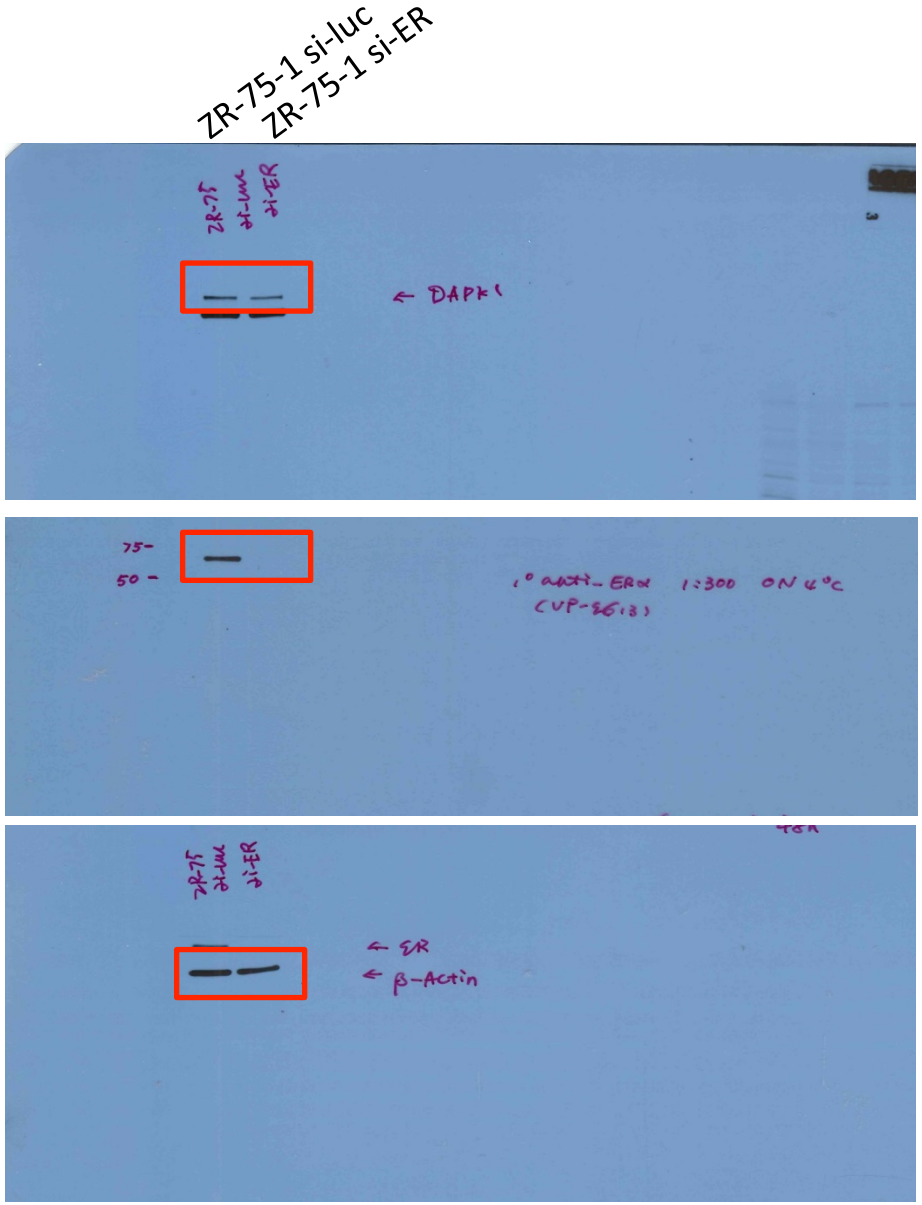

DAPK-1

ER

β-actin

Figure S2C

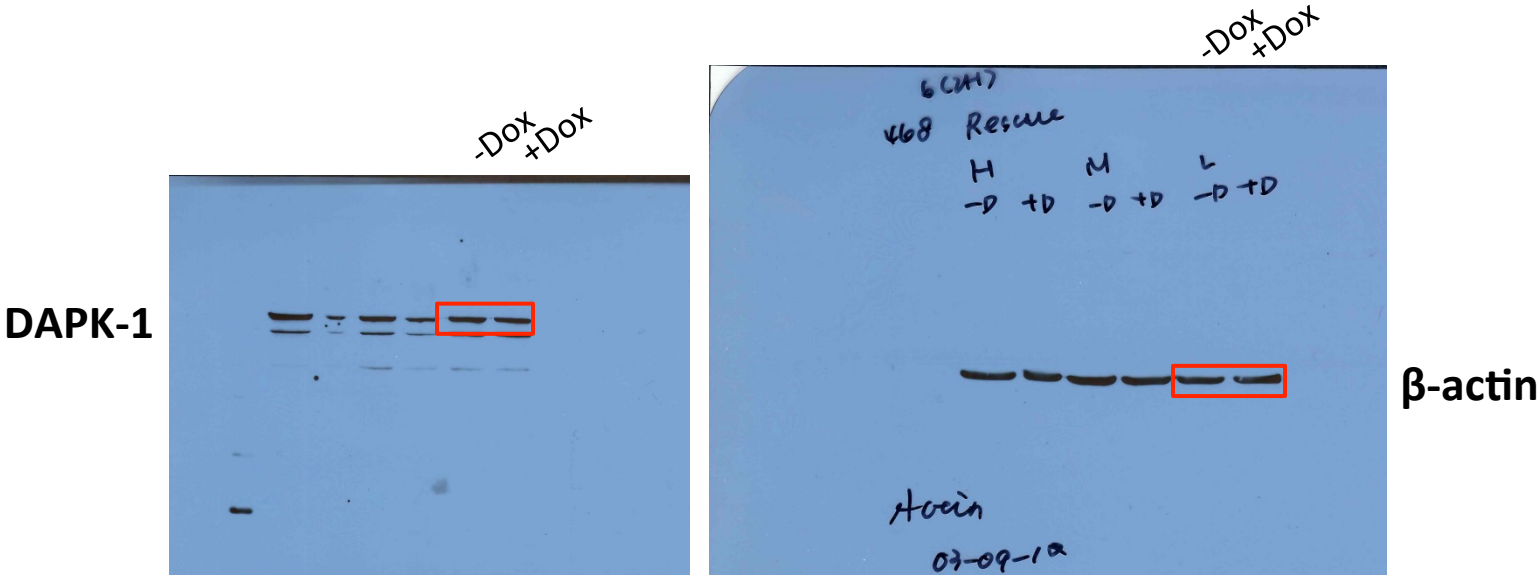

Figure S2I

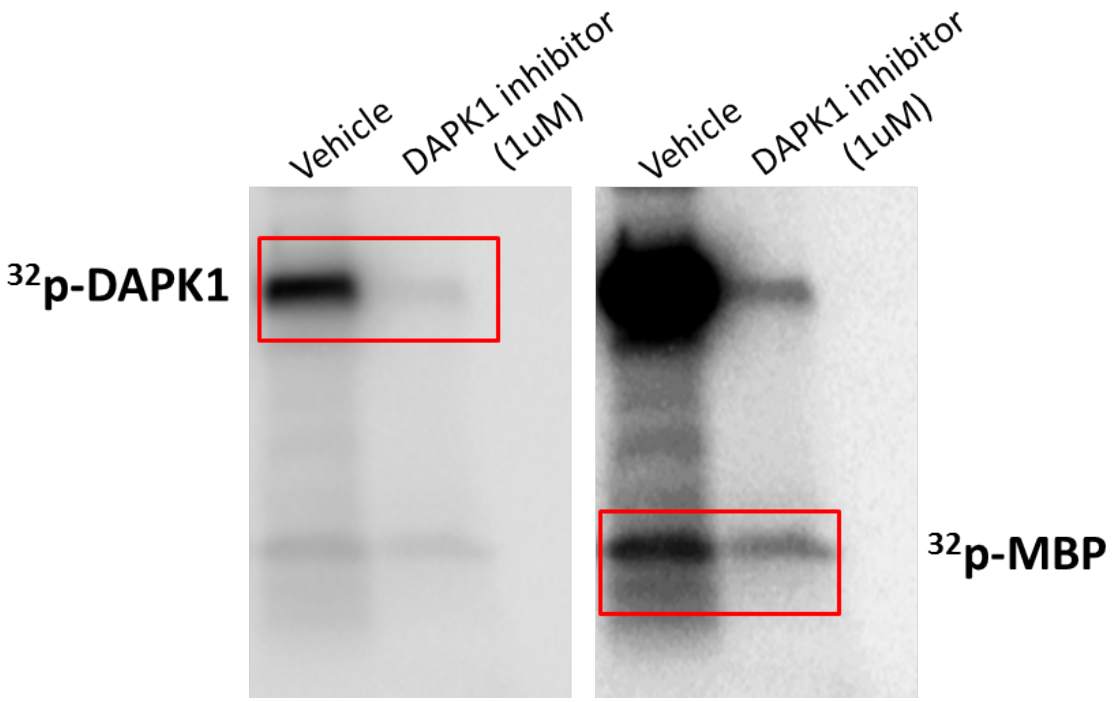
Vehicle
DAPK1 inhibitor (1uM)
Vehicle
DAPK1 inhibitor (1uM)
32p-DAPK1
32p-MBP

Figure S4B

IB:TSC2

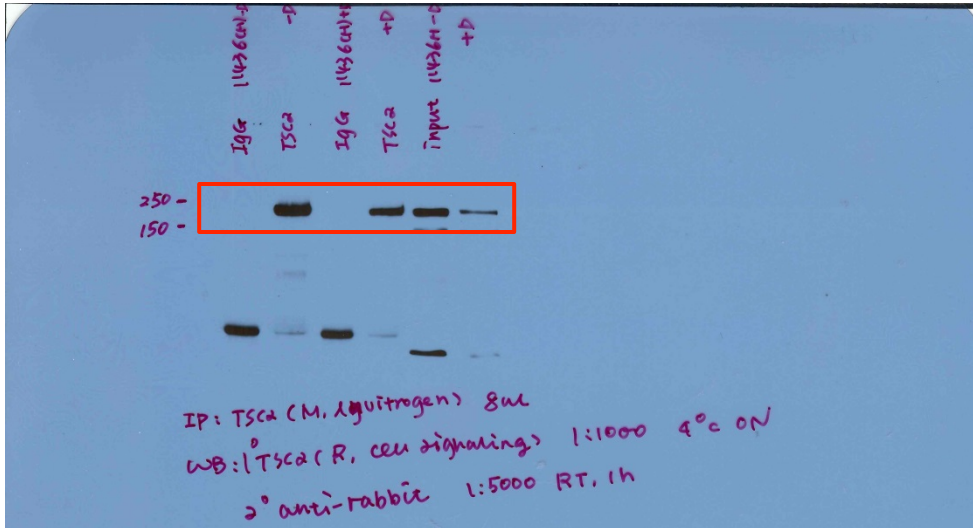

IB:TSC1

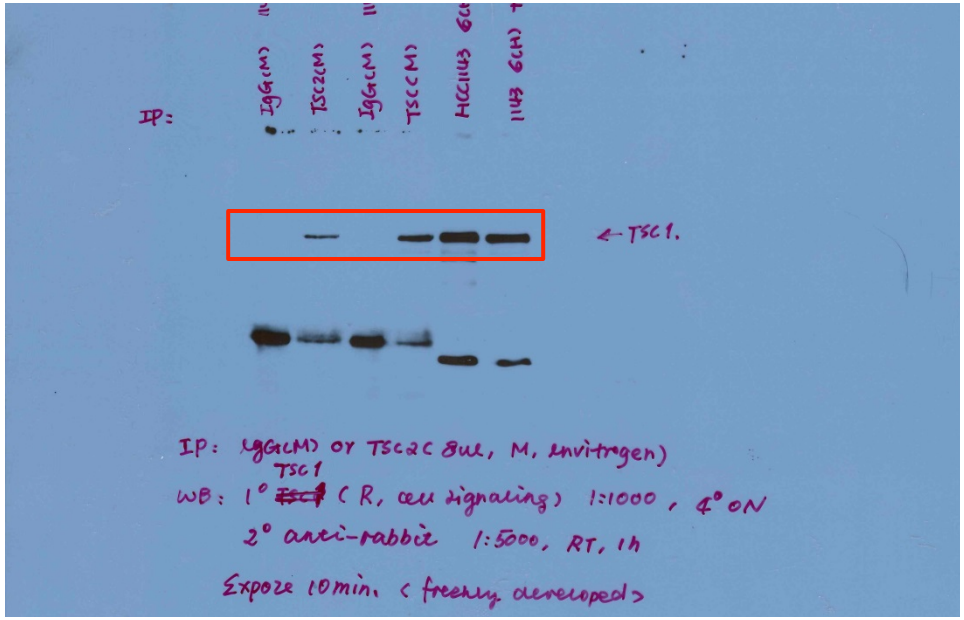

Figure S4C

IB:TSC2

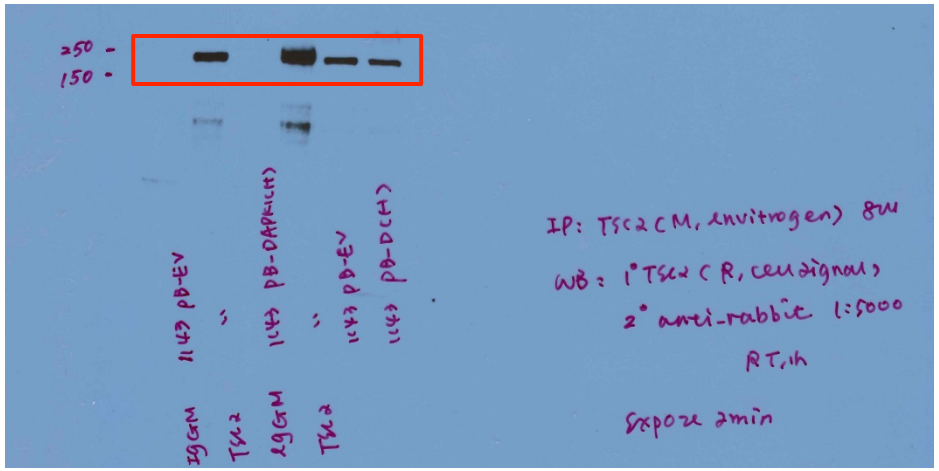

IB:TSC1

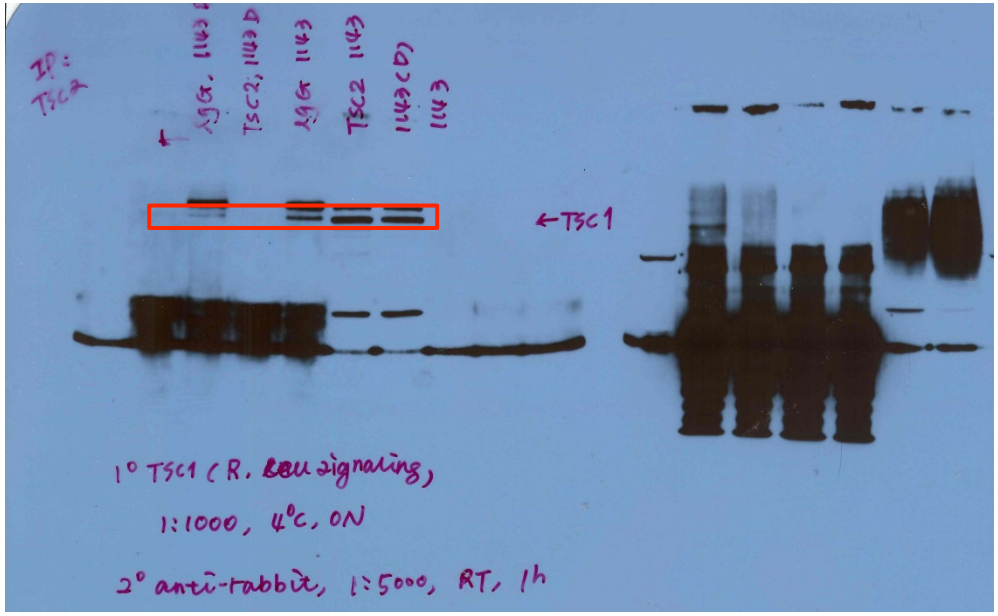

Figure S4D

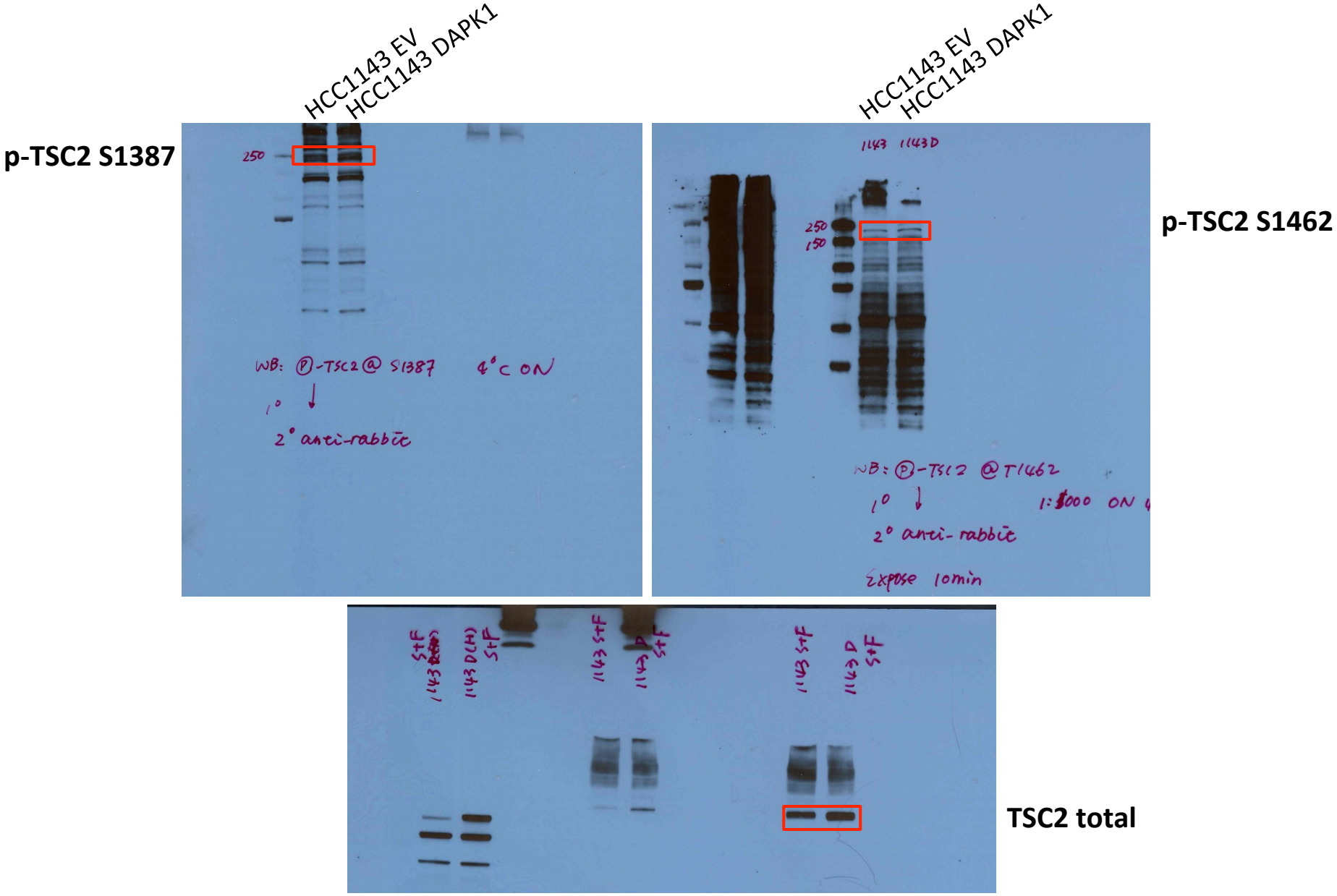
HCC1143 EV
HCC1143 DAPK1
p-TSC2 S1387
250
WB: Ⓟ-TSC2 @ S1387 4°C ON
1°
2° anti-rabbit
HCC1143 EV
HCC1143 DAPK1
1143 1143D
250
150
p-TSC2 S1462
WB: Ⓟ-TSC2 @ T1462
1°
1:1000 ON
2° anti-rabbit
Expose 10min
TSC2 total

Figure S4E

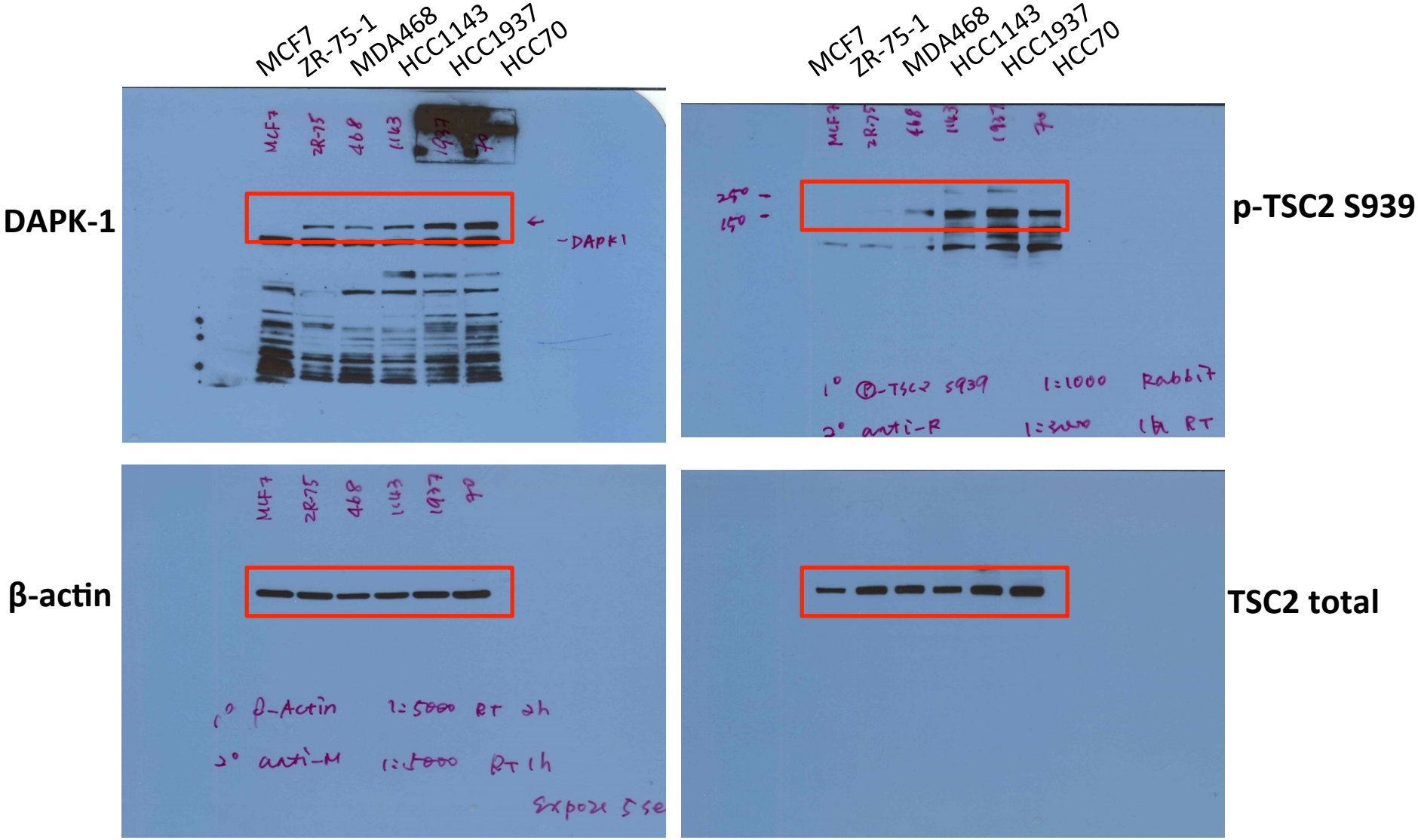
MCF7
ZR-75-1
MDA468
HCC1143
HCC1937
HCC70
DAPK-1
-DAPK1
MCF7
ZR-75
468
1143
1937
70
250
150
1° P-TSC2 S939 1:1000 Rabbit
2° anti-R
1h RT
p-TSC2 S939
β-actin
1° β-Actin 1:5000 RT 2h
2° anti-M 1:5000 RT 1h
Expoz 5 se
TSC2 total

Figure S4F

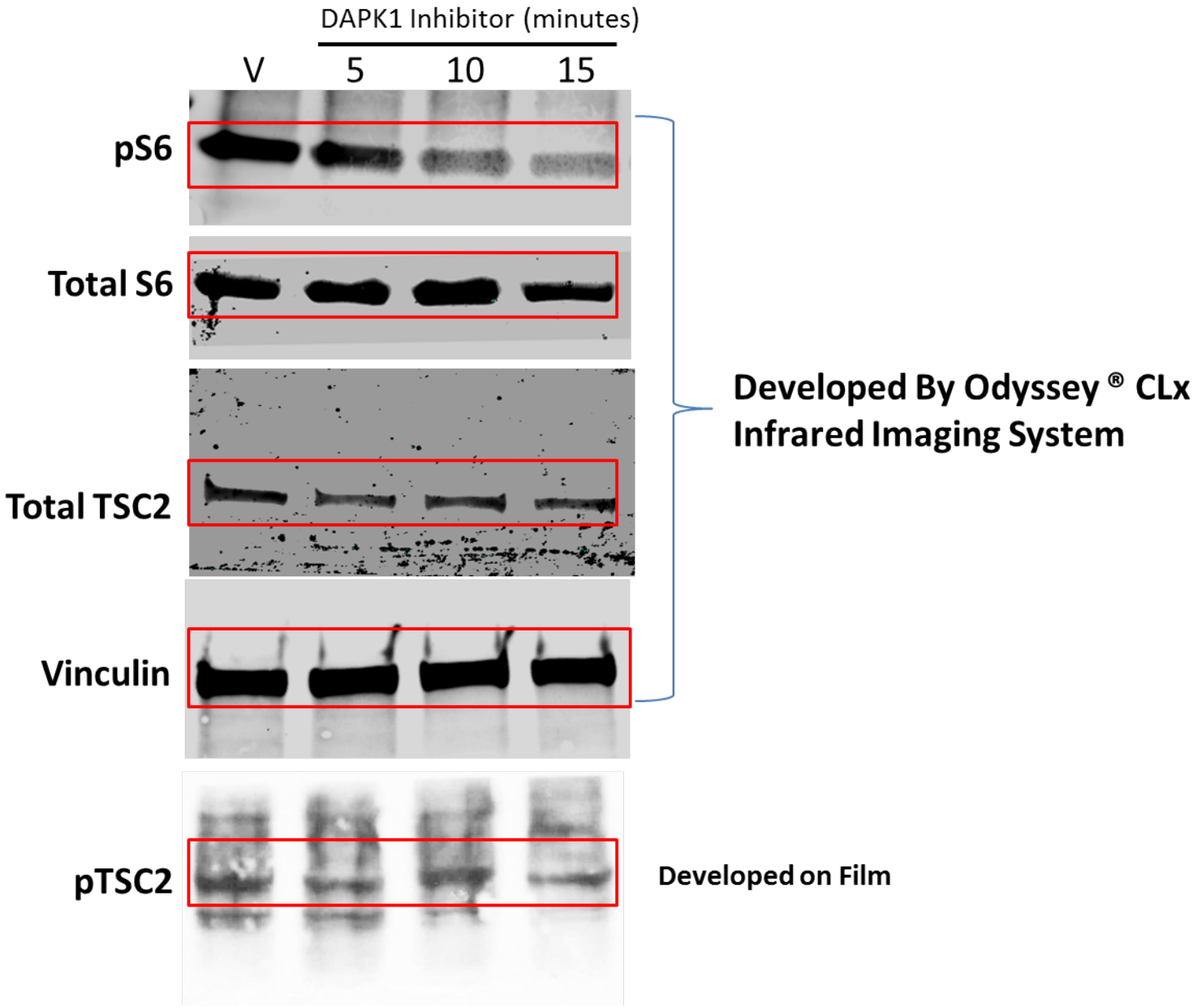
DAPK1 Inhibitor (minutes)
V
5
10
15
pS6
Total S6
Total TSC2
Vinculin
pTSC2
Developed By Odyssey ® CLx Infrared Imaging System
Developed on Film